GlueX-doc-1784
SVN: docs/GlueXdoc/prod_bcal_guides
Draft: June 6, 2011
Original: June 17, 2011

Acceptance Studies for the Production Light Guides of the BCAL

E.S. Smith

1 Introduction

The light guides for the Barrel Calorimeter (BCAL) will be trapezoidal shapes connecting the output face of the BCAL modules to the SiPM light sensors. Similar light guides have been studied previously [1]. However, the geometry was not finalized and the present task is to optimize some parameters and characterize the light guides that will be used in the actual detector. The light collection was simulated using GEANT3 [2] in a procedure described in more detail in previous notes [1, 3, 4, 5]. The trajectories of light rays through the light guide were propagated using the standard PHYS260 package for "Cerenkov Photons." The photons that are relevant to this study are in the visible spectrum but the optical properties from the "Cerenkov" package cover this part of the spectrum as well. The parameters of the materials are the same as those described previously, if not specified here.

2 Setup and Geometry

The production geometry is azimuthally symmetric, consisting of four identical radial columns per BCAL module. Each column consists of ten light guides, which cover an azimuthal angle of 1.875° degrees. Both the input and output faces of the light guides are trapezoidal in shape. The bases of the guide are glued to the face of the BCAL and grow in width toward the outer edge of the module. The height of the bases is 20.57 cm for the inner six guides and 24.64 cm for the outer four. The base of the guide receives the light from the calorimeter and funnels it down to a smaller trapezoid covering the sensitive area of the SiPM sensors, which is 1.27×1.27 cm^2. The nominal length of the light guides is 8 cm. There is a 0.5 mm air gap between the output of the light guide and the 0.45 mm clear epoxy protective coating [1] over the sensitive area of the SiPM. An example of the light guide shapes is shown in

[1] We use the optical properties of acrylic for the coating material.

Table 1: Sizes of the ten production light guides for the Bcal. The trapezoid dimensions are denoted using the notation (bottom-top × height).

Configuration	Input Trapezoid (mm^2)	Length (cm)	Output Trapezoid (mm^2)	Eff (%)
g1	20.96-21.64 × 20.57	8	13.19-13.61 × 13.19	0.748
g2	21.64-22.30 × 20.57	8	13.19-13.61 × 13.19	0.723
g3	22.30-22.99 × 20.57	8	13.19-13.61 × 13.19	0.701
g4	22.99-23.65 × 20.57	8	13.19-13.61 × 13.19	0.683
g5	23.67-24.33 × 20.57	8	13.19-13.61 × 13.19	0.662
g6	24.33-25.02 × 20.57	8	13.19-13.61 × 13.19	0.643
g7	25.02-25.83 × 24.64	8	13.19-13.61 × 13.19	0.516
g8	25.83-26.62 × 24.64	8	13.19-13.61 × 13.19	0.503
g9	26.64-27.43 × 24.64	8	13.19-13.61 × 13.19	0.488
g10	27.46-27.84 × 24.64	8	13.19-13.61 × 13.19	0.477

Fig. 1, which shows several views of light guide #6 (g6), and some optical rays traced through the volume. The dimensions for the ten guides are given in Table 1.

The collection efficiencies were calculated for an input distribution of light rays which was uniform over the entrance area and uniform in $\cos\theta$ up to the maximum trapping angle θ_{max} in the fiber of 26.7°. The effective attenuation length in the light guide was set to 240 cm. An optical ray reaching the sensitive SiPM volume is reported as the successful detection of a photon. For each configuration studied, we produced a series of histograms that display the collection acceptance and uniformity, and where losses occur for that geometry. Figs. 2-8 show representative plots for light guide g1, Figs. 9-15 show the plots for g6 and Figs. 16-22 show the results for g10. These plots are for the output face height of 1.32 cm, which was chosen after an optimization study described in the next section.

3 Acceptance studies

3.1 Size of output face

We first studied the acceptance of the light geometries as a function of the size of their output face. This face is positioned in front of the SiPM across a 0.5 mm air gap. Light exiting the light guide around the perimeter of the output face can be lost when the light rays are bent away from the SiPM. However, making the area smaller

increases the likelihood of rays being reflected back from the air interface. Therefore, there is a maximum in the collection efficiency, as shown in Fig. 23. The peaking is most prominent for the smaller light guides, whereas the light guides from the outer layers (7–10) show very little dependence on the output size. The maximum could be chosen in the range of 1.3 to 1.4 cm We select the output height to be 13.2 mm in order to maintain the maximum clearance between light guides.

3.2 Length of light guide

The length of the light guide was varied for light guide g6 to study the acceptance as a function of length. The acceptance is essentially independent of the length of the light guide, changing from 64.0% at 8 cm down to 63.5% at 12 cm (see Table 2). Reducing the length below 8 cm was not considered to ensure that most of the light rays bounce at least once as they travel down the light guide and destroy any correlations between the input and output positions. Therefore, the length of the light guide is fixed at 8 cm.

3.3 Features for monitoring attachments

Several suggestions have been made for attaching monitoring LEDs to the light guide. The most recent proposals [6] include machining a step into one side of the light guide, which may be used to support the PC board as well as position the LED, and machining a small trench to place the LED. These two schemes were modeled to estimate the effect these features may have on acceptance.

The step was modeled as shown in Fig. 24 as a horizontal cut with a 2.8 mm step near the base of the light guide. Surprisingly, NKUA had measured no loss of acceptance for the step feature within the accuracy of their measurements. Our simulations confirm that observation, which we calculate to be 62%. However, we also find that the acceptance becomes very non-uniform, as shown in Fig. 25. The acceptance at the top is reduced when light rays impinge on the side of the step, but are compensated by increased acceptance of rays that bounce off the bottom of the step at a shallow angle increasing their chances of being accepted. We find that the acceptance varies between 72% and 48% along the vertical dimension, which is unacceptable.

The trench scheme is not very developed and was modeled by simply applying a black patch to the top of the light guide, as shown in Fig. 28. Note that in the figure only the opaque bottom of the solid is relevant to the optics, which absorbs any light rays that impinge on it. In all likelihood the trench would actually extend into the light guide by a few millimeters, but the effect on light collection will be similar to simply absorbing any light rays that hit that area. The patch reduces the

Table 2: Collection efficiency for various trapezoidal configurations. Two scenarios for attachments of monitoring LEDs are considered. The trapezoid dimensions are denoted using the notation (bottom-top × height).

Configuration	Length (cm)	Monitoring Feature	Eff (%)
g6	8	None	64.3
g6	9.6	None	64.0
g6	12	None	63.5
g6	8	step (3mm)	60.5
g6	8 8	patch 0.24 cm^2 (0.17-0.30× 1 cm^2)	63.7
g6	8 8	patch 0.94 cm^2 (0.33-0.61× 2 cm^2)	61.8

acceptance by about 2.7%/cm^2 of obscured area. As shown in Fig. 27 this creates a small non-uniformity but is small as long as the affected area is also small.

3.4 Flat region at the base

The nominal design (Fig. 28) includes a flat section near the base of the light guide to aid mechanical support and aid in gluing. We find, however, that these facets have a very similar effect as the step feature studied earlier: they create non-uniformities in the collection efficiency. This is shown in Figs. 29-36. The acceptance varies between 80% and 62% between the perimeter and center of the light guide. The region affected depends on the height of the flat section, but the difference in acceptance remains even for very low flat facets. The best option for performance is to eliminate the flat section altogether.

4 Summary and conclusions

We have studied the light collection for the production geometry of Bcal light guides. The production geometry is azimuthally symmetric, consisting of four identical radial columns per BCAL module. Each column consists of ten light guides, which cover an azimuthal angle of 1.875° degrees. Both the input and output faces of the light guides are trapezoidal in shape. The dimensions for the ten guides are given in Table 1. We have studied the light collection as a function of the size of the output face and

concluded that the optimum size of the trapezoid is 1.3.2-1.3.6 $\times$ 1.32 (bottom-top $\times$ height). The light collection is insensitive to the length of the light guide and we have confirmed the length of 8 cm.

We have also studied the effect of various schemes for attaching the monitoring LEDs to the surface. We conclude that the "step" option results in large non-uniformities in the collection efficiency and therefore should not be implemented. Features added to the light guide of approximately 1 cm^2 in size should affect the light collection by only a couple of percent and are acceptable changes to the geometry.

Finally we have investigated the impact of having short flat facets at the base before beginning the taper of the sides of the light guide to help mechanical support and gluing. The effect of these flat surfaces is to create acceptance non-uniformities at the edges of the light guide, which we would like to avoid. We therefore recommend that the light guides begin the taper immediately at the base of the light guide. This might require additional fixtures to assist in gluing the light guides to the calorimeter, but will also reduce any cross talk between channels.

References

[1] E.S. Smith. Trapezoidal guides for the light collection for sipms. GlueX-doc-1432, 2010. 1

[2] Computing CERN Application Software Group and Networks Division. Geant detector description and simulation tool. http://wwwasd.web.cern.ch/wwwasd/geant, 1993. 1

[3] E.S. Smith. Light guide collection for the bcal outer layers. GlueX-doc-959, 2008. 1

[4] E.S. Smith. Light collection for light guides for use with fine mesh pmts for the bcal readout. GlueX-doc-1077, 2008. 1

[5] E.S. Smith. Reference calculations for light collection for light collection for fine mesh pmts. GlueX-doc-1287, 2009. 1

[6] C. Kourkoumelis, G. Voulgaris, and Stratos. Calorimeter Working Group Meeting, May 24, 2011. http://www.jlab.org/Hall-D/software/wiki/index.php/May_24%2C_2011_Calorimetry, 2011. 3

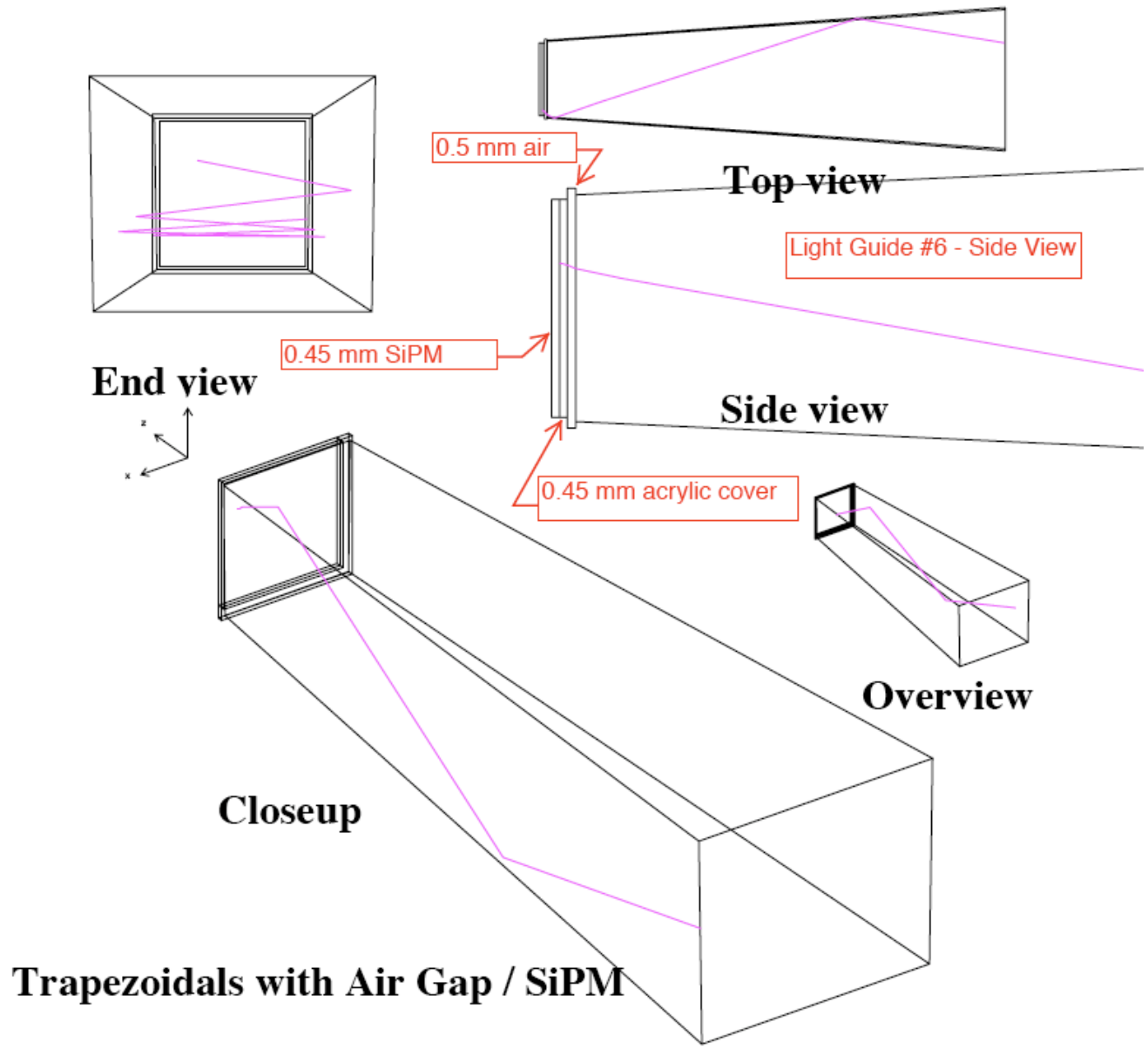

Figure 1: Various views of the geometry for light guide #6, including rays traced through the guide. The middle right shows an enlarged side view of the output face, including a 0.5 mm air gap, acrylic cover (actually glue) of the SiPM and the SiPM active face itself.

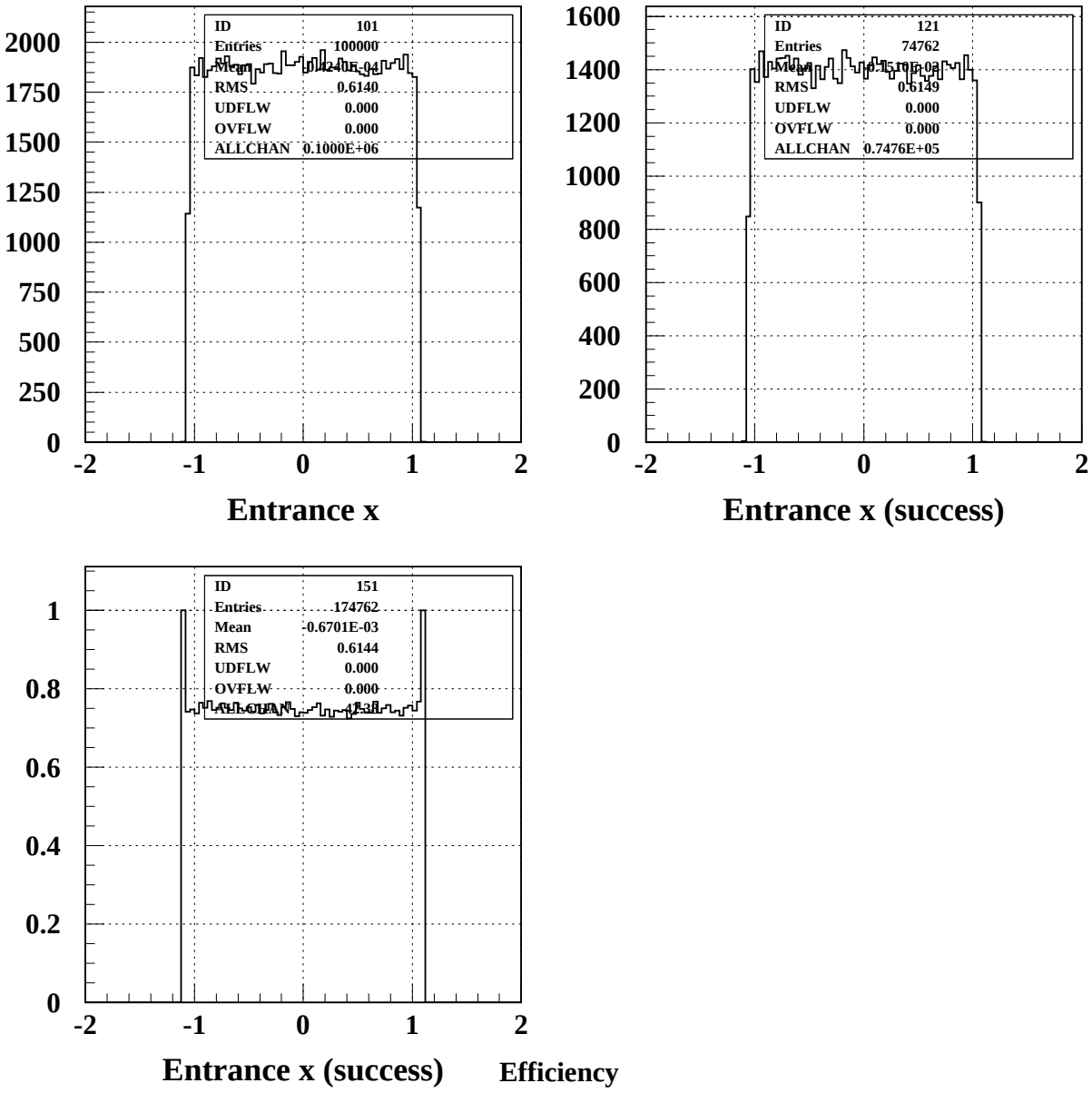

Figure 2: Light Guide #1. Top left) Horizontal distribution of rays at the entrance. Top right) Horizontal distribution of rays that reach the SiPM. Bottom left) Acceptance as a function of horizontal position.

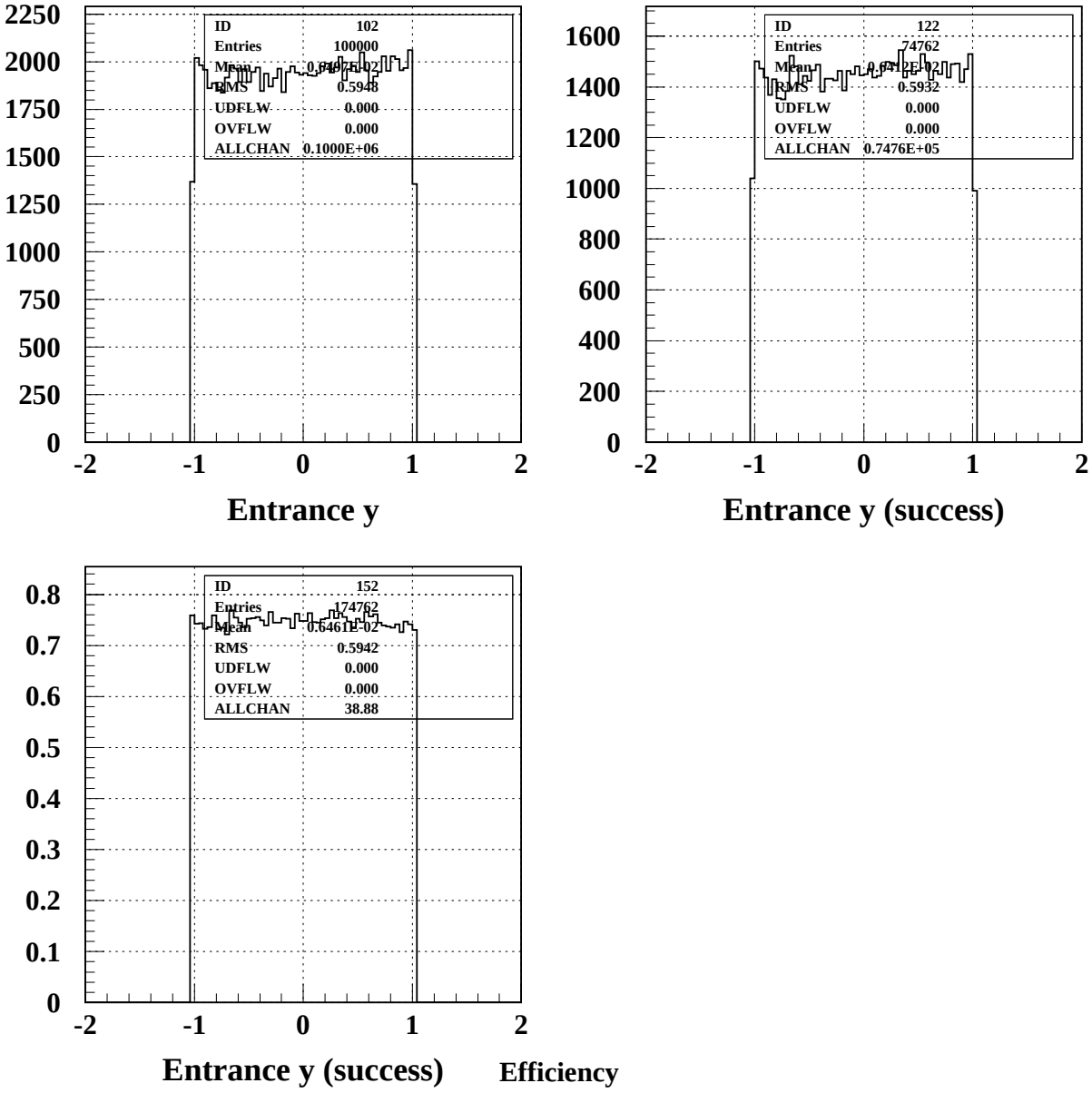

Figure 3: Light Guide #1. Top left) Vertical distribution of rays at the entrance. Top right) Vertical distribution of rays that reach the SiPM. Bottom left) Acceptance as a function of vertical position.

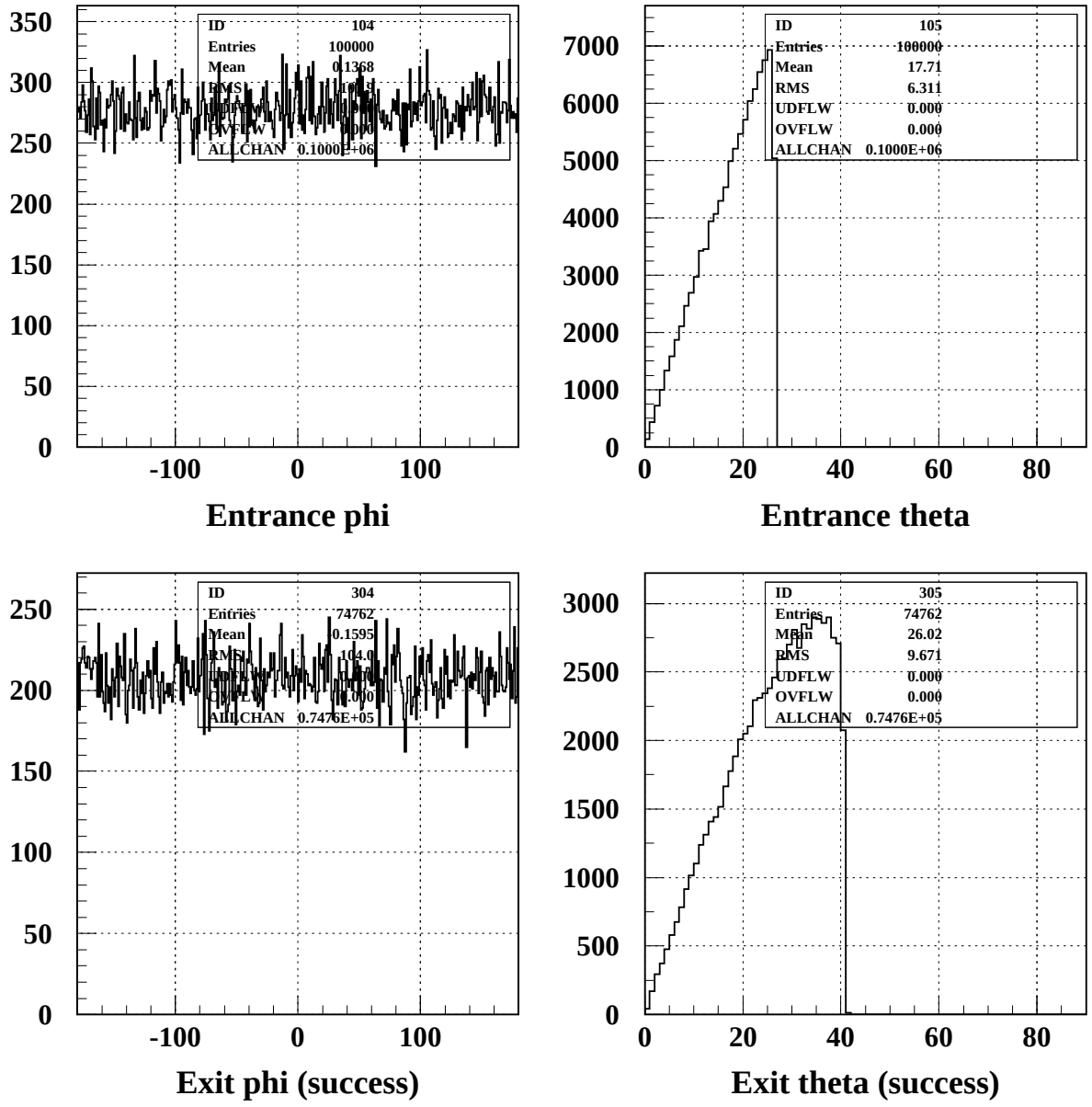

Figure 4: Light Guide #1. Top left) Azimuthal angle distribution at entrance. Top right) Polar angle distribution at entrance. Bottom left) Azimuthal angle distribution at SiPM. Bottom right) Polar angle distribution at SiPM.

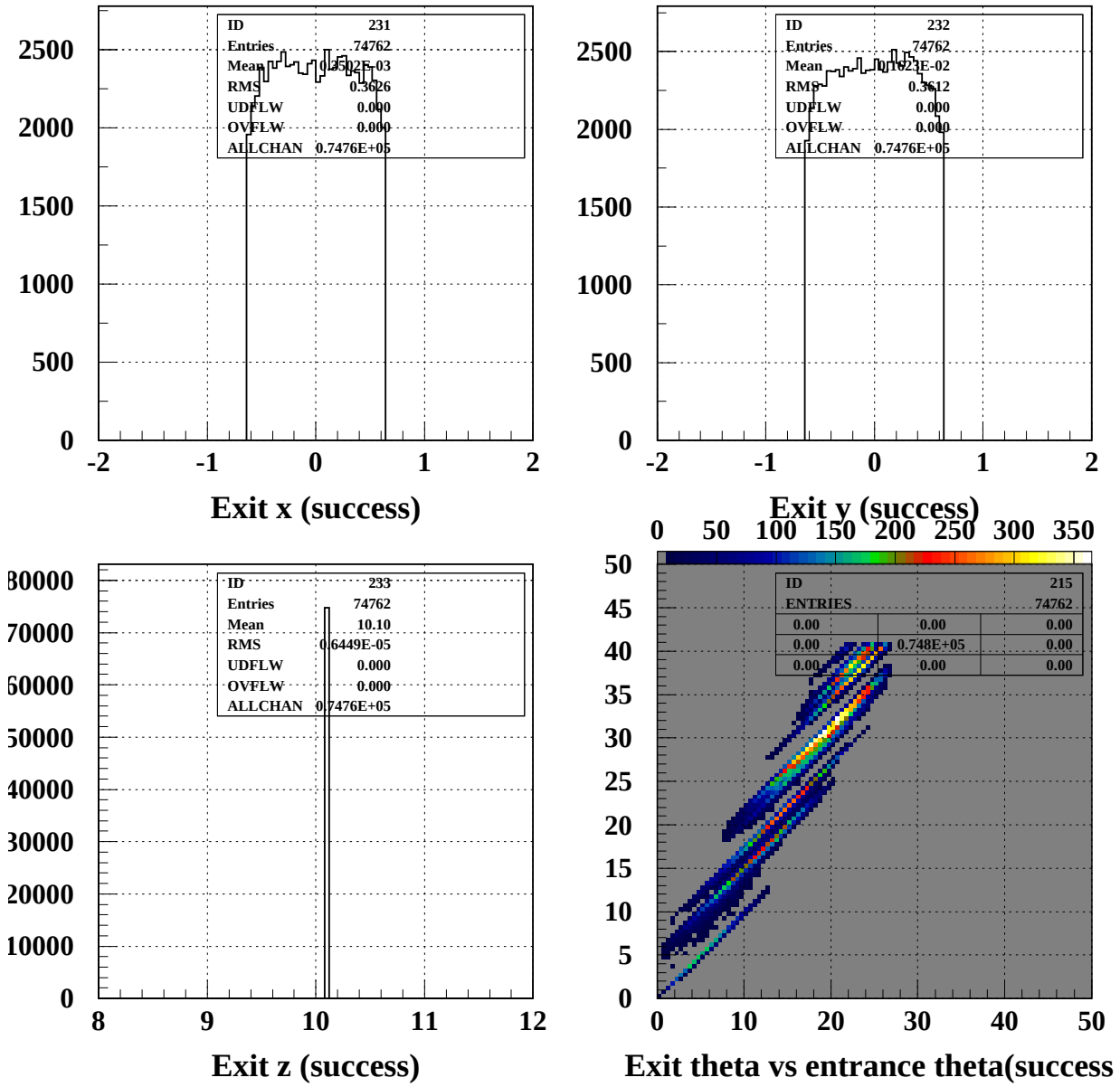

Figure 5: Light Guide #1. Top left) Horizontal distribution at the SiPM Top right) Vertical distribution at the SiPM. Bottom left) Longitudinal position at the SiPM. Bottom right) Polar angle at SiPM vs. polar angle at entrance. Three major bands indicate zero, one, two and three reflections.

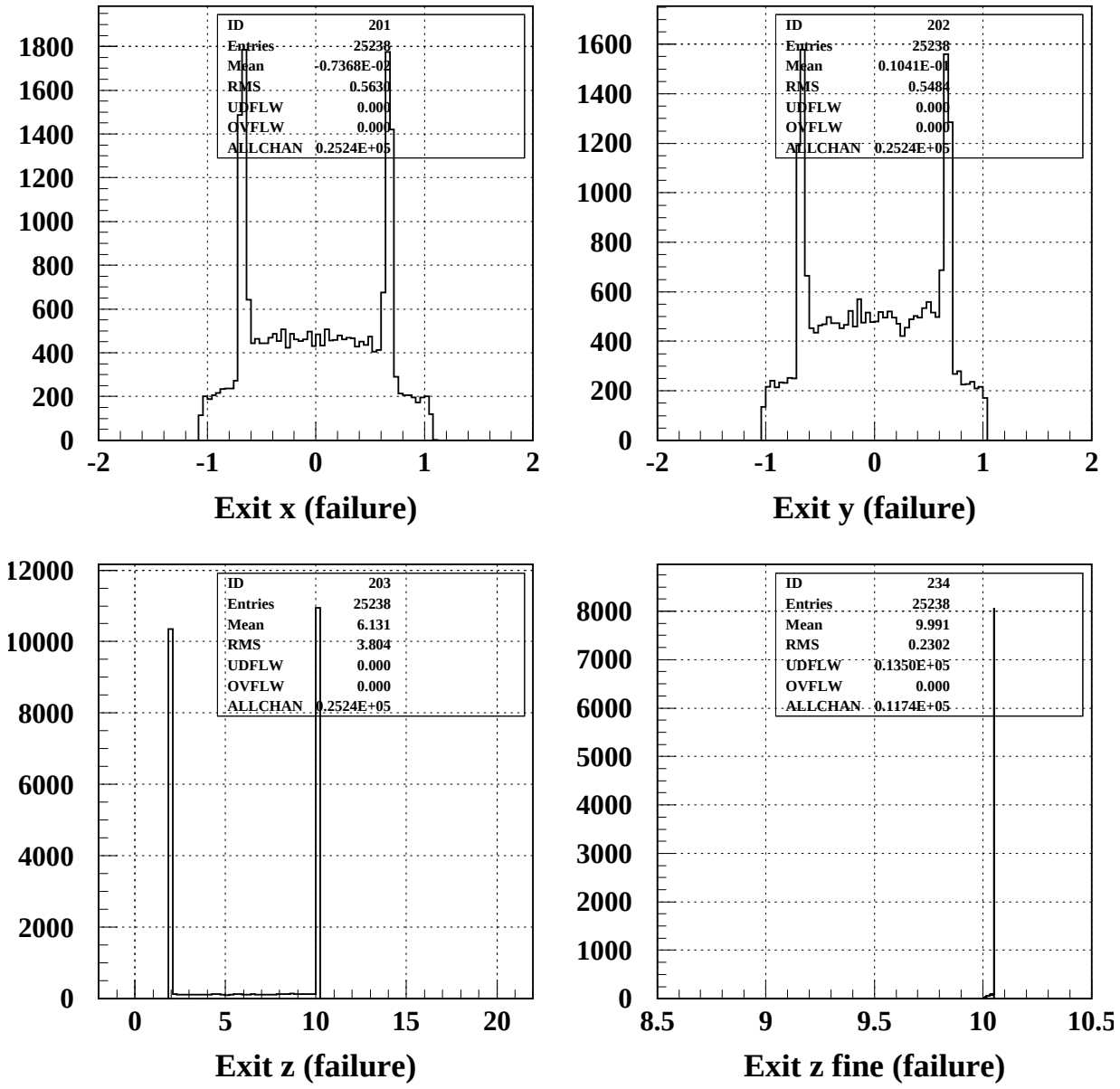

Figure 6: Light Guide #1. Top left) Horizontal distribution of rays that fail to reach the SiPM Top right) Vertical distribution of rays that fail to reach the SiPM. Bottom left) Longitudinal distribution of particles that fail to reach the SiPM. Bottom right) Same as previous on a finer scale.

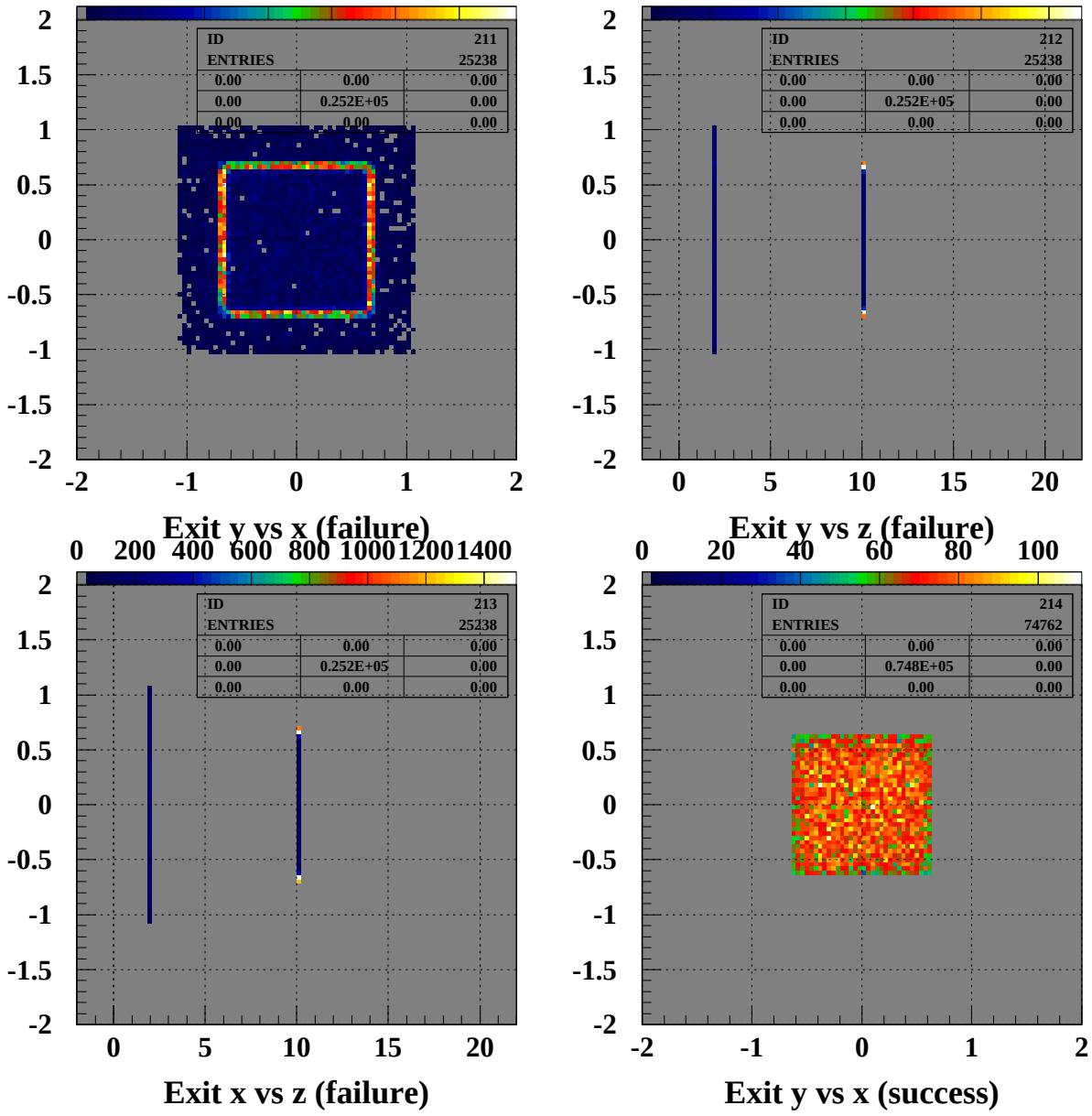

Figure 7: Light Guide #1. Top left) Vertical vs horizontal positions for rays that fail. Top right) Vertical vs longitudinal positions for rays that fail. Bottom left) Horizontal vs longitudinal positions of rays that fail. Bottom right) Vertical vs horizontal positions at the SiPM.

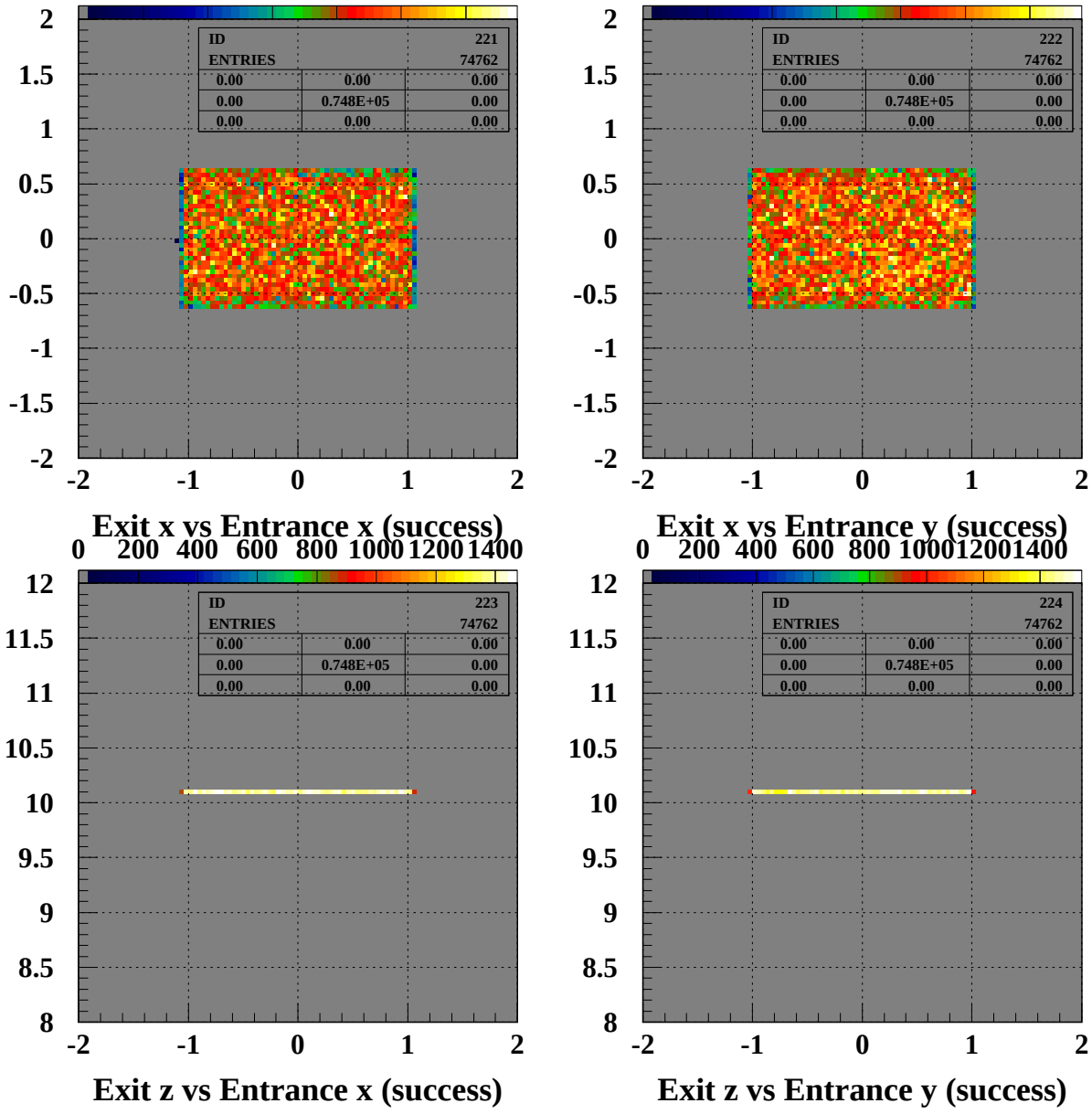

Figure 8: Light Guide #1. Top left) Correlation of horizontal position between entrance and exit. Top right) Correlation of vertical position between entrance and exit. Bottom left) Exit z vs entrance x. Bottom right) Exit z vs entrance y.

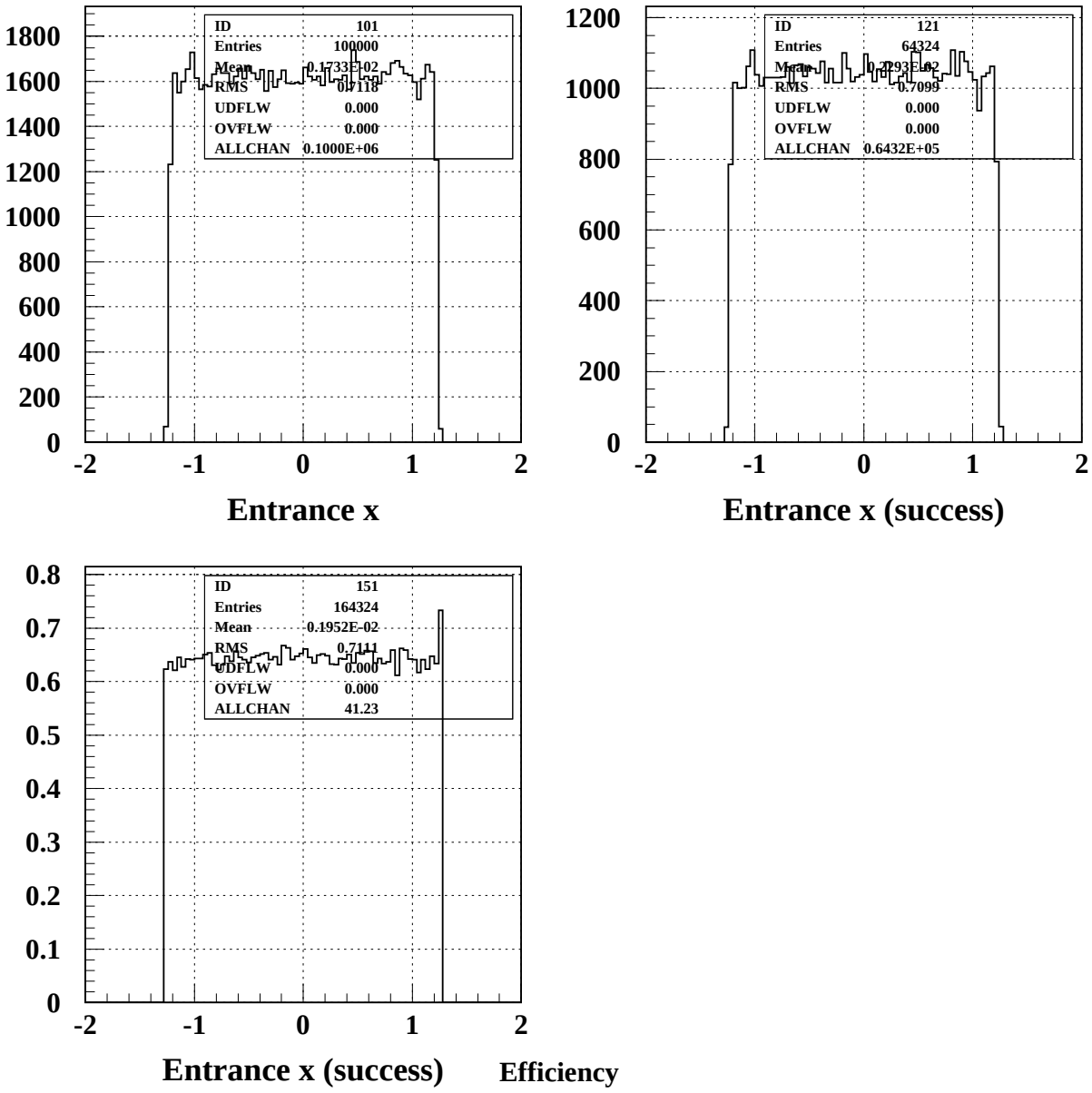

Figure 9: Light Guide #6. Top left) Horizontal distribution of rays at the entrance. Top right) Horizontal distribution of rays that reach the SiPM. Bottom left) Acceptance as a function of horizontal position.

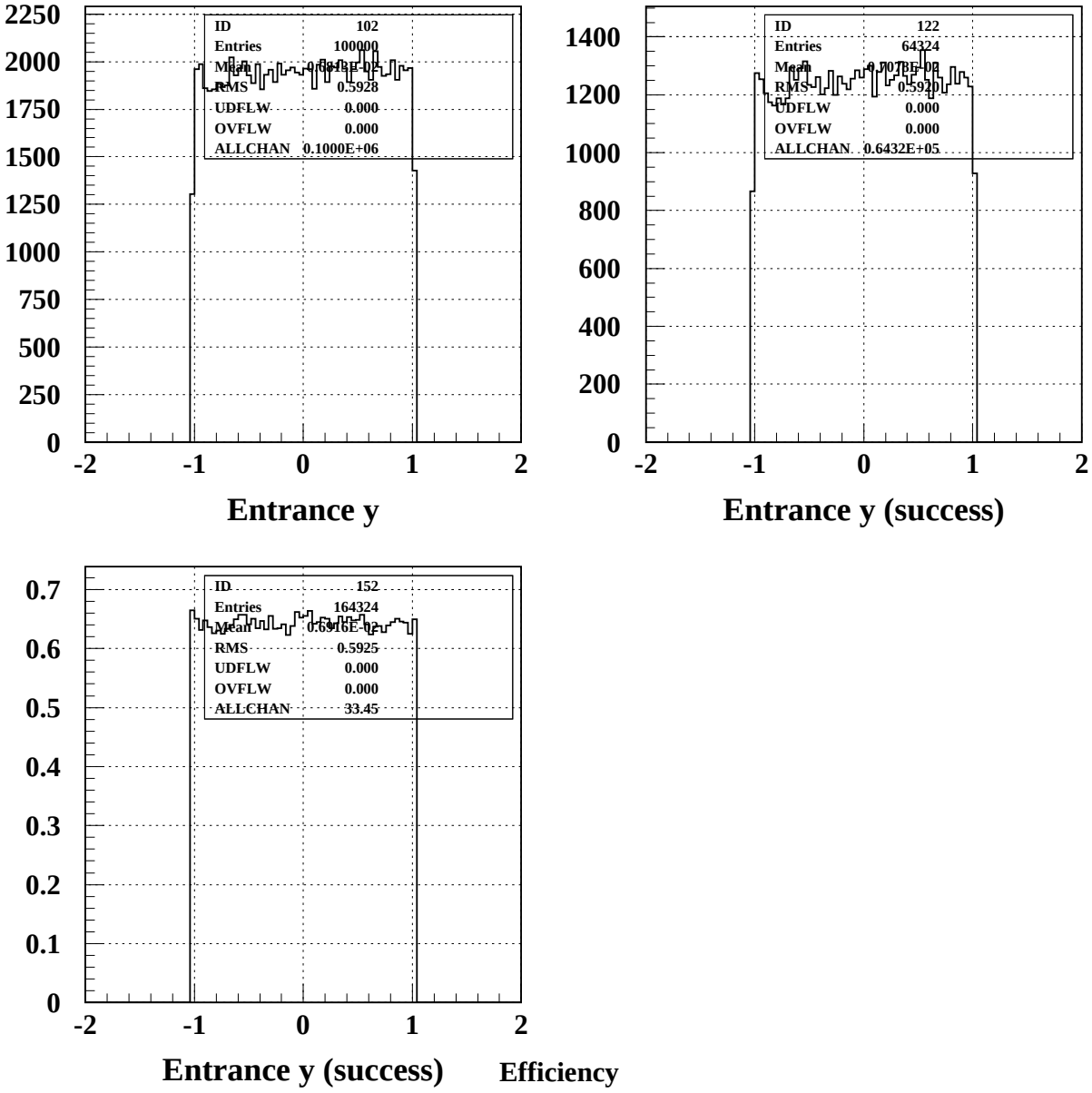

Figure 10: Light Guide #6. Top left) Vertical distribution of rays at the entrance. Top right) Vertical distribution of rays that reach the SiPM. Bottom left) Acceptance as a function of vertical position.

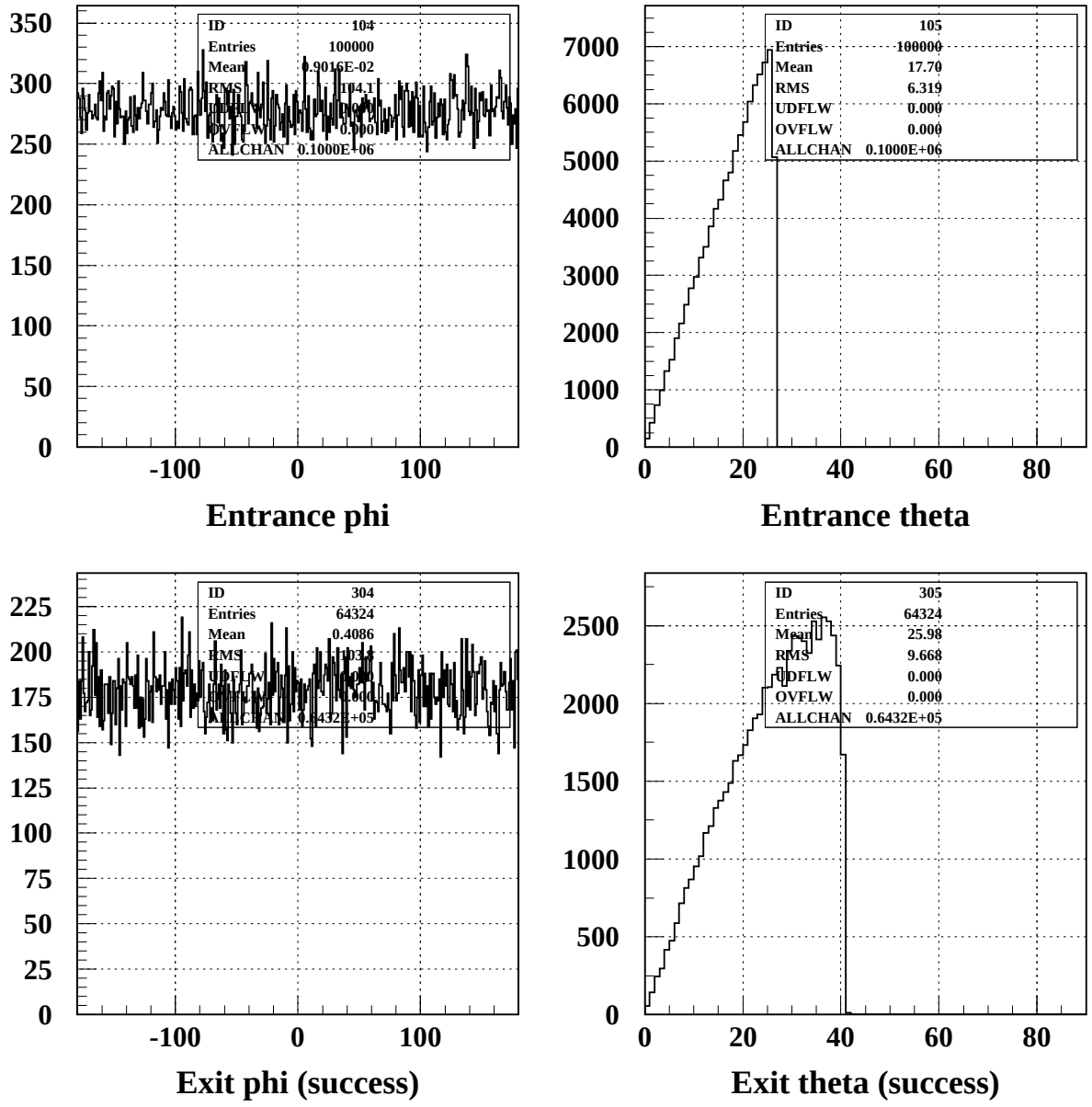

Figure 11: Light Guide #6. Top left) Azimuthal angle distribution at entrance. Top right) Polar angle distribution at entrance. Bottom left) Azimuthal angle distribution at SiPM. Bottom right) Polar angle distribution at SiPM.

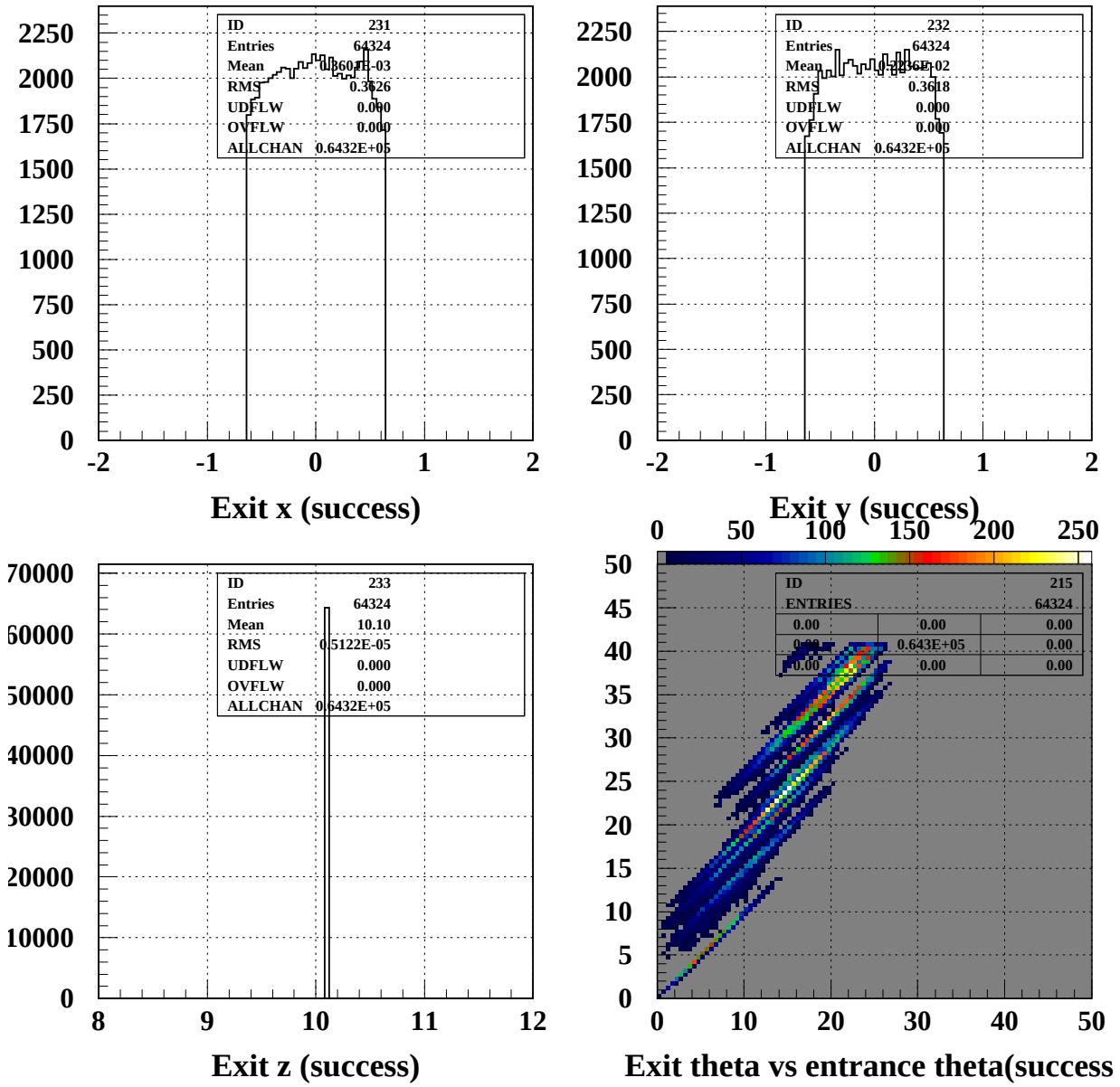

Figure 12: Light Guide #6. Top left) Horizontal distribution at the SiPM Top right) Vertical distribution at the SiPM. Bottom left) Longitudinal position at the SiPM. Bottom right) Polar angle at SiPM vs. polar angle at entrance. Three major bands indicate zero, one, two and three reflections.

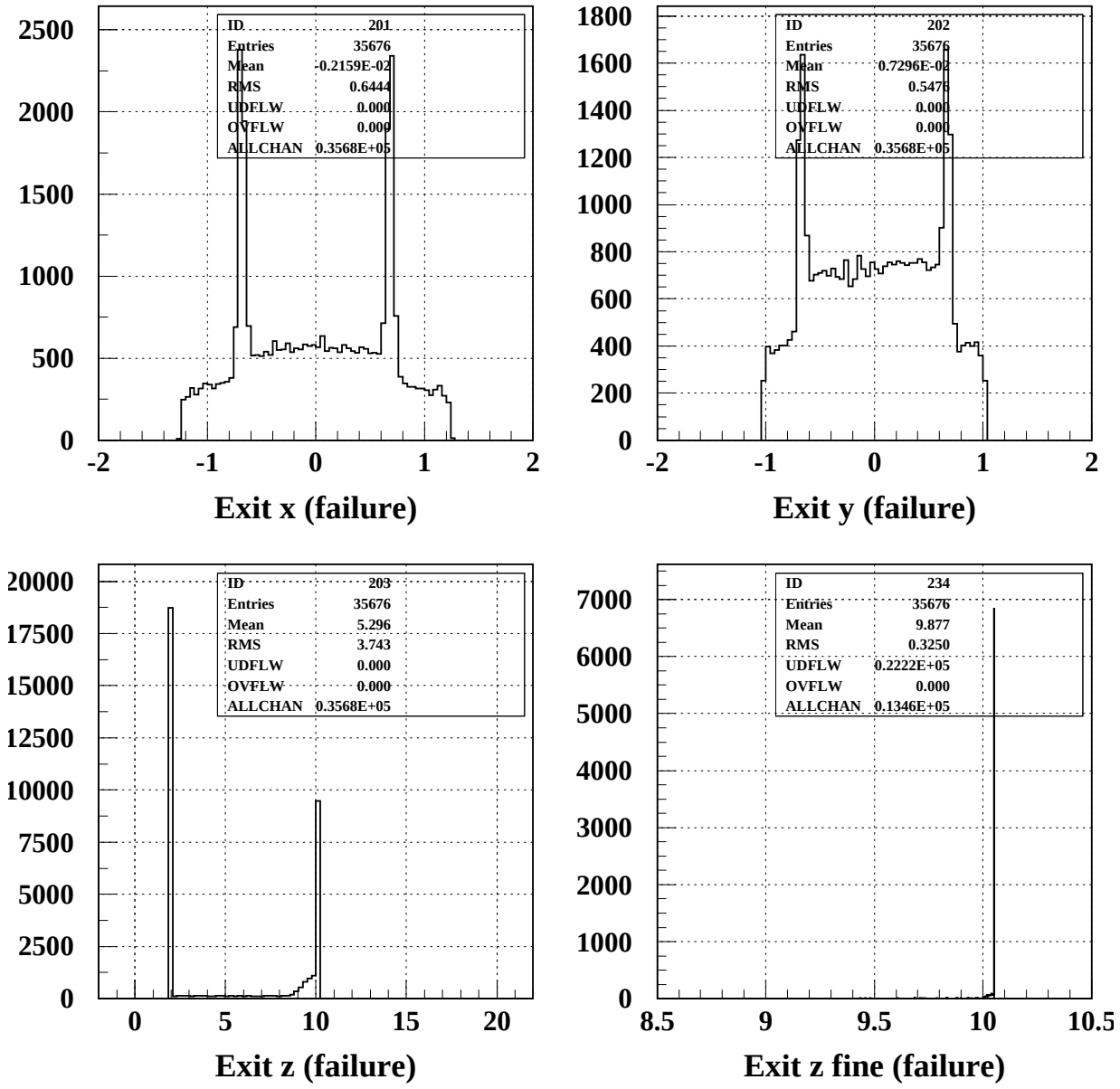

Figure 13: Light Guide #6. Top left) Horizontal distribution of rays that fail to reach the SiPM Top right) Vertical distribution of rays that fail to reach the SiPM. Bottom left) Longitudinal distribution of particles that fail to reach the SiPM. Bottom right) Same as previous on a finer scale.

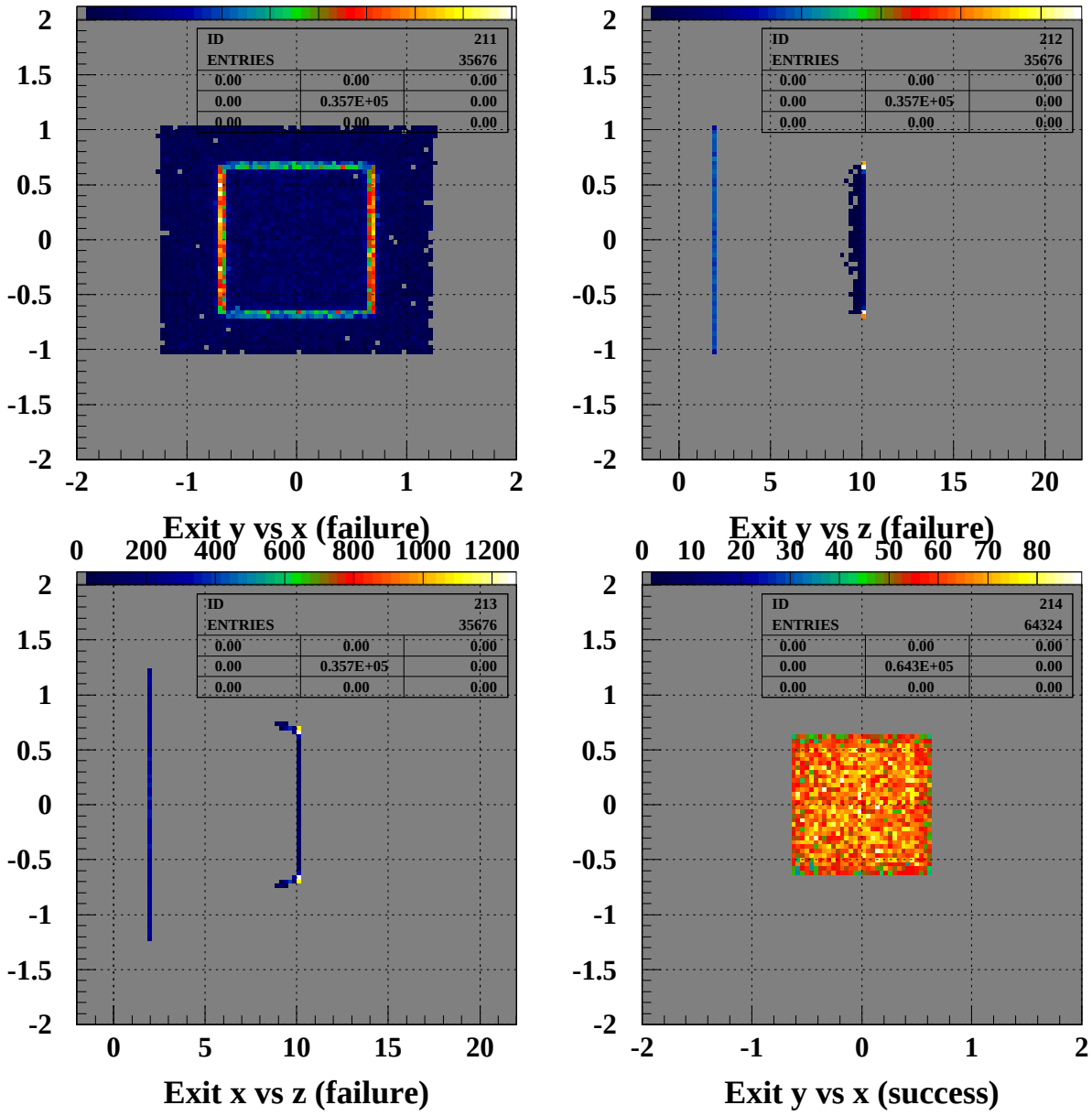

Figure 14: Light Guide #6. Top left) Vertical vs horizontal positions for rays that fail. Top right) Vertical vs longitudinal positions for rays that fail. Bottom left) Horizontal vs longitudinal positions of rays that fail. Bottom right) Vertical vs horizontal positions at the SiPM.

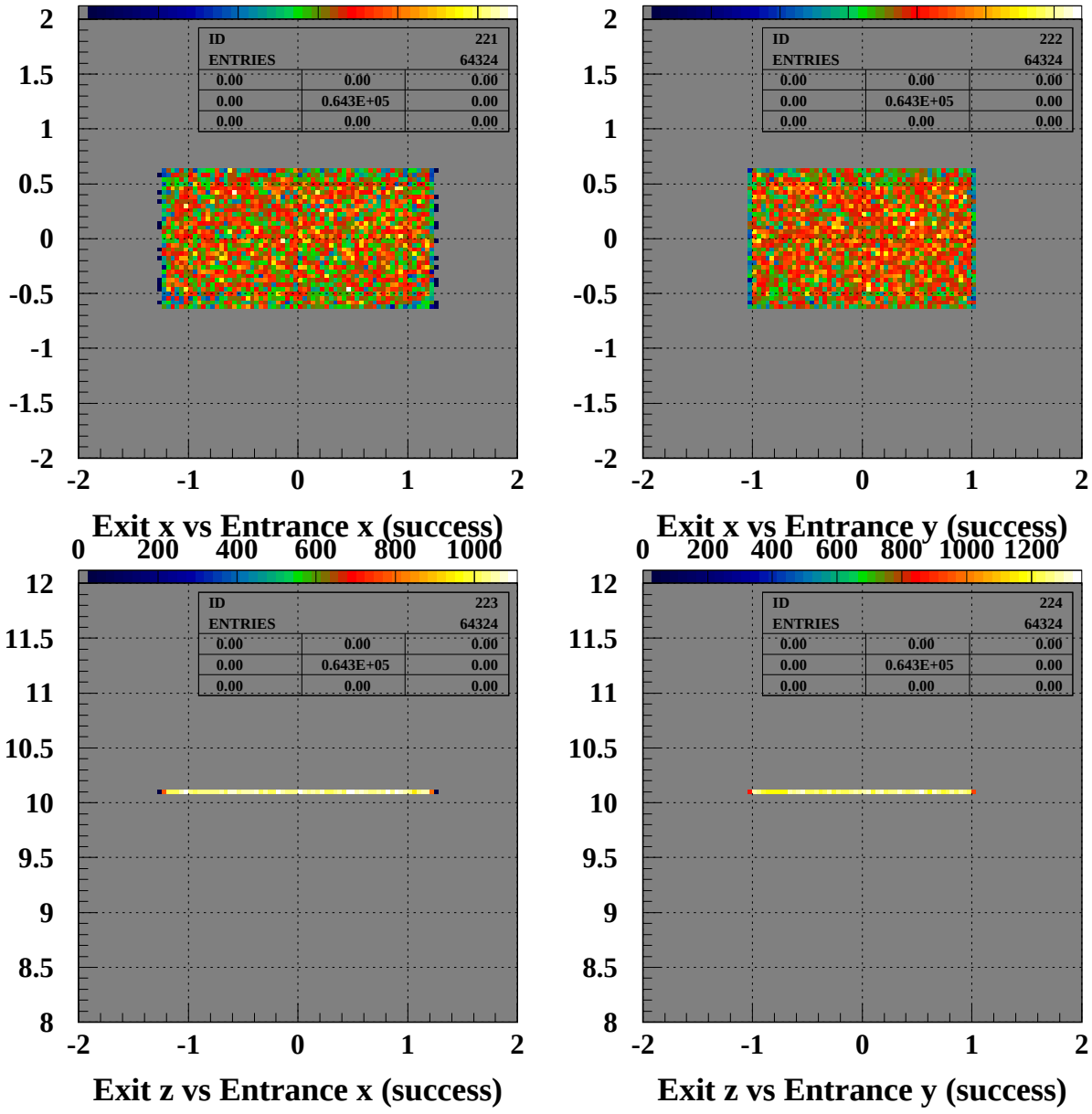

Figure 15: Light Guide #6. Top left) Correlation of horizontal position between entrance and exit. Top right) Correlation of vertical position between entrance and exit. Bottom left) Exit z vs entrance x. Bottom right) Exit z vs entrance y.

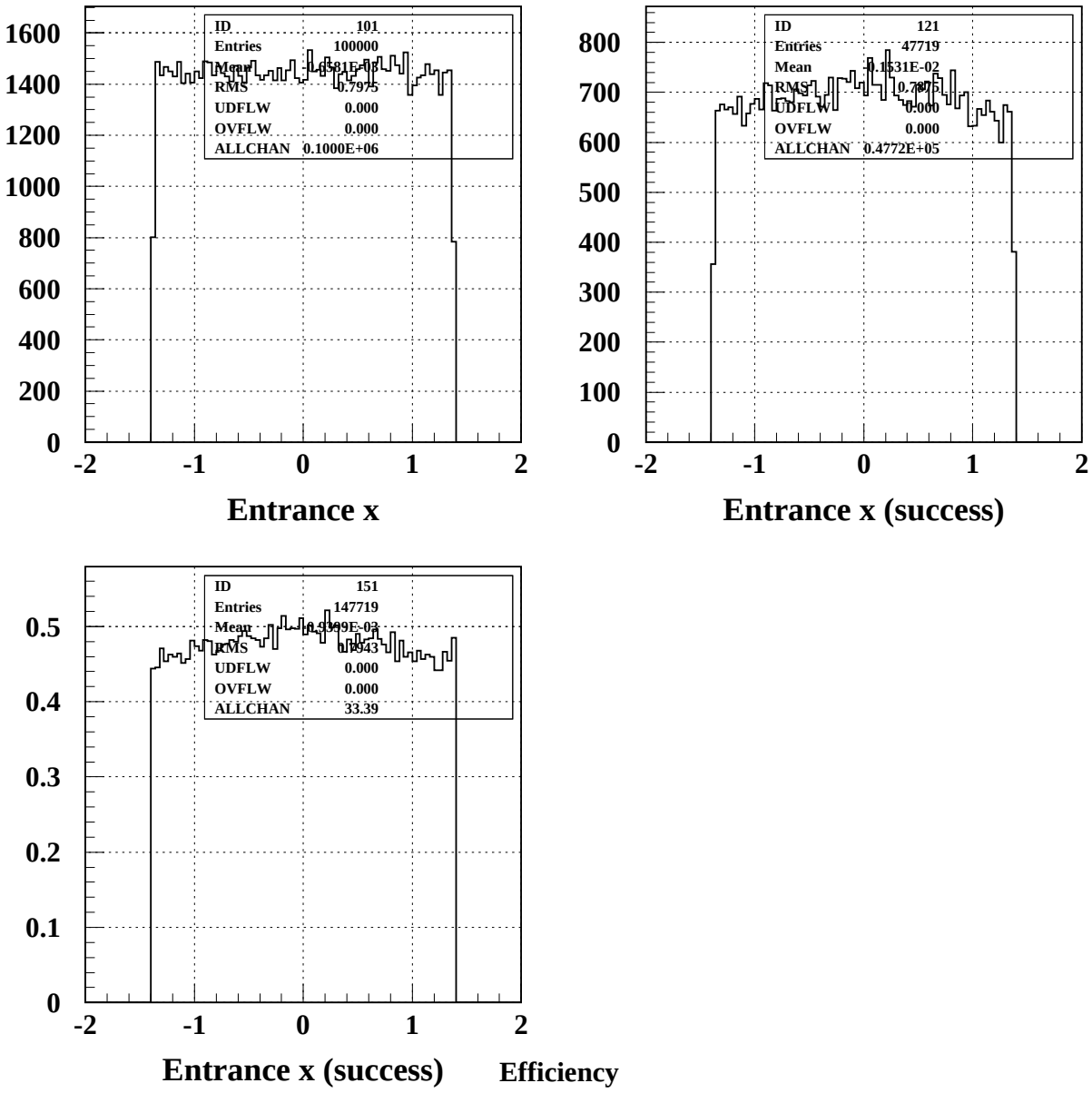

Figure 16: Light Guide #10. Top left) Horizontal distribution of rays at the entrance. Top right) Horizontal distribution of rays that reach the SiPM. Bottom left) Acceptance as a function of horizontal position.

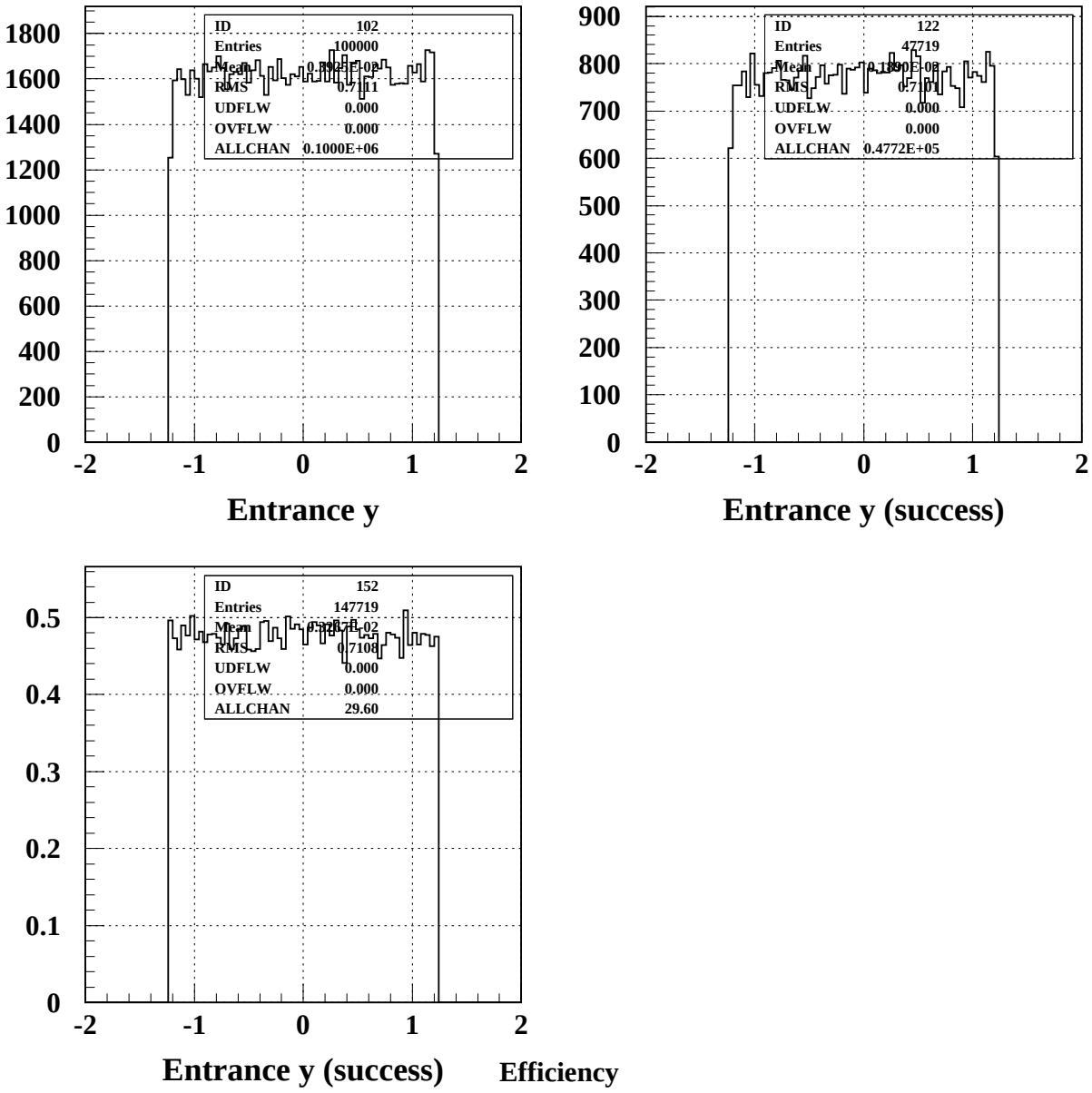

Figure 17: Light Guide #10. Top left) Vertical distribution of rays at the entrance. Top right) Vertical distribution of rays that reach the SiPM. Bottom left) Acceptance as a function of vertical position.

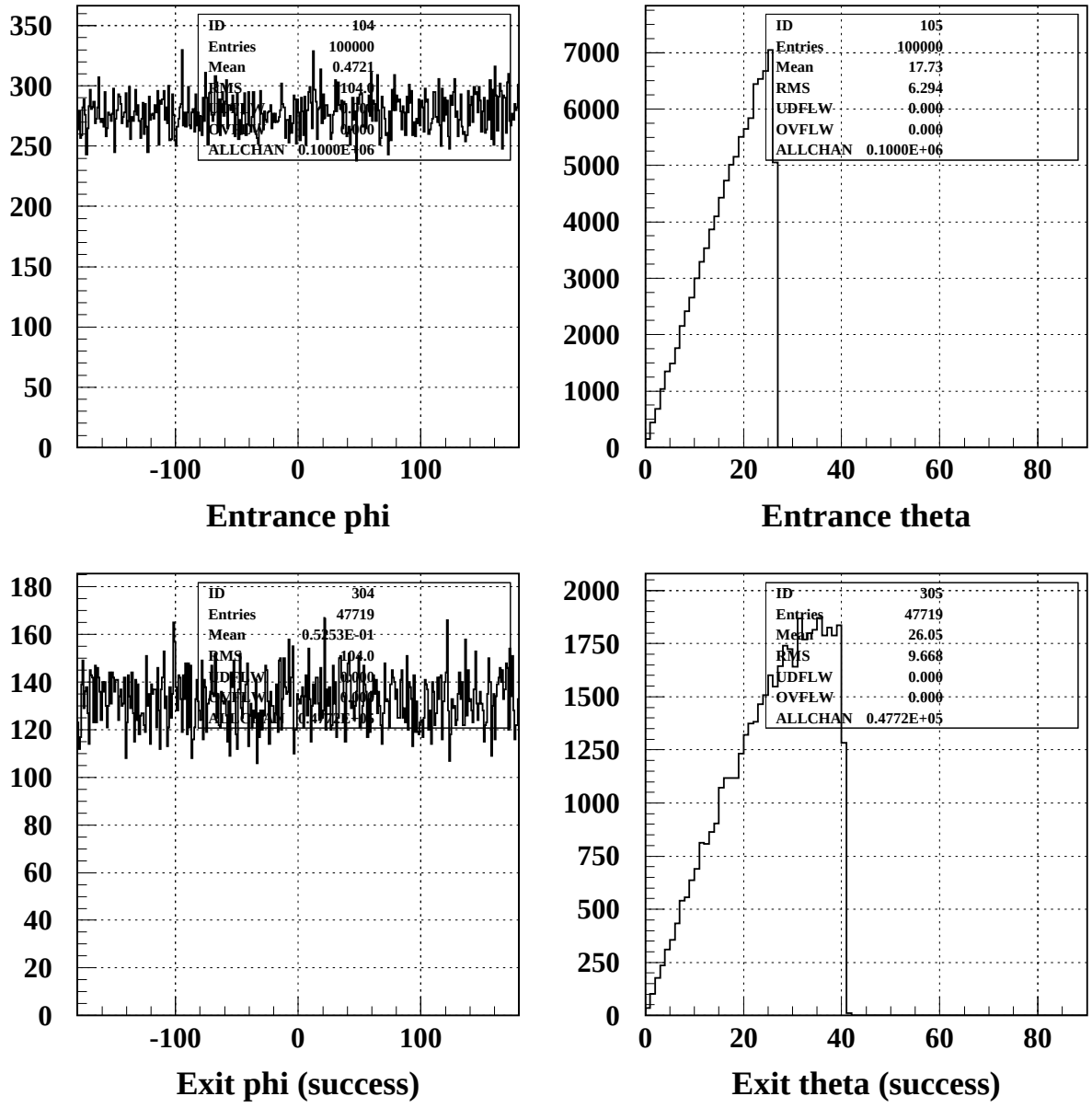

Figure 18: Light Guide #10. Top left) Azimuthal angle distribution at entrance. Top right) Polar angle distribution at entrance. Bottom left) Azimuthal angle distribution at SiPM. Bottom right) Polar angle distribution at SiPM.

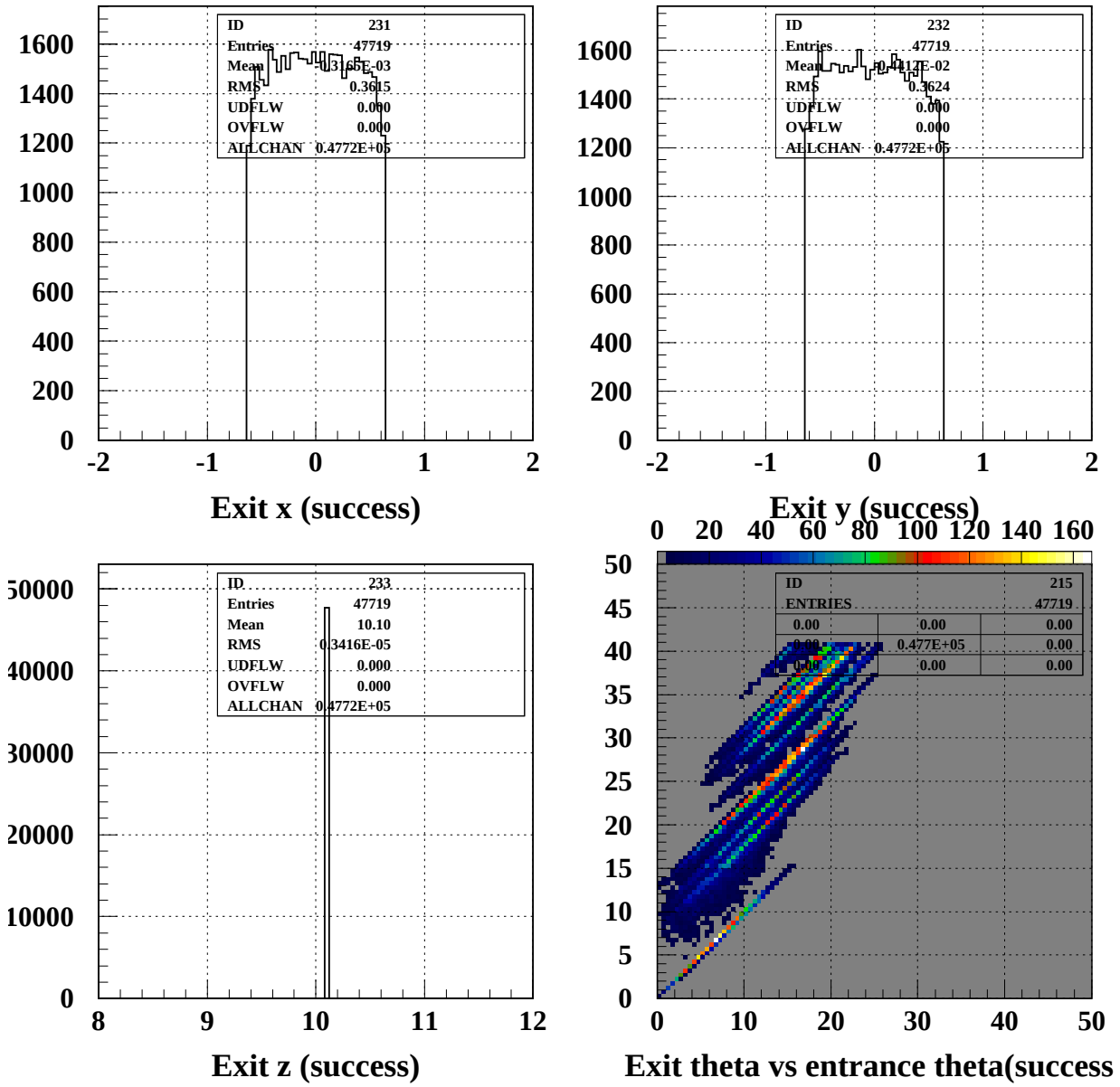

Figure 19: Light Guide #10. Top left) Horizontal distribution at the SiPM Top right) Vertical distribution at the SiPM. Bottom left) Longitudinal position at the SiPM. Bottom right) Polar angle at SiPM vs. polar angle at entrance. Three major bands indicate zero, one, two and three reflections.

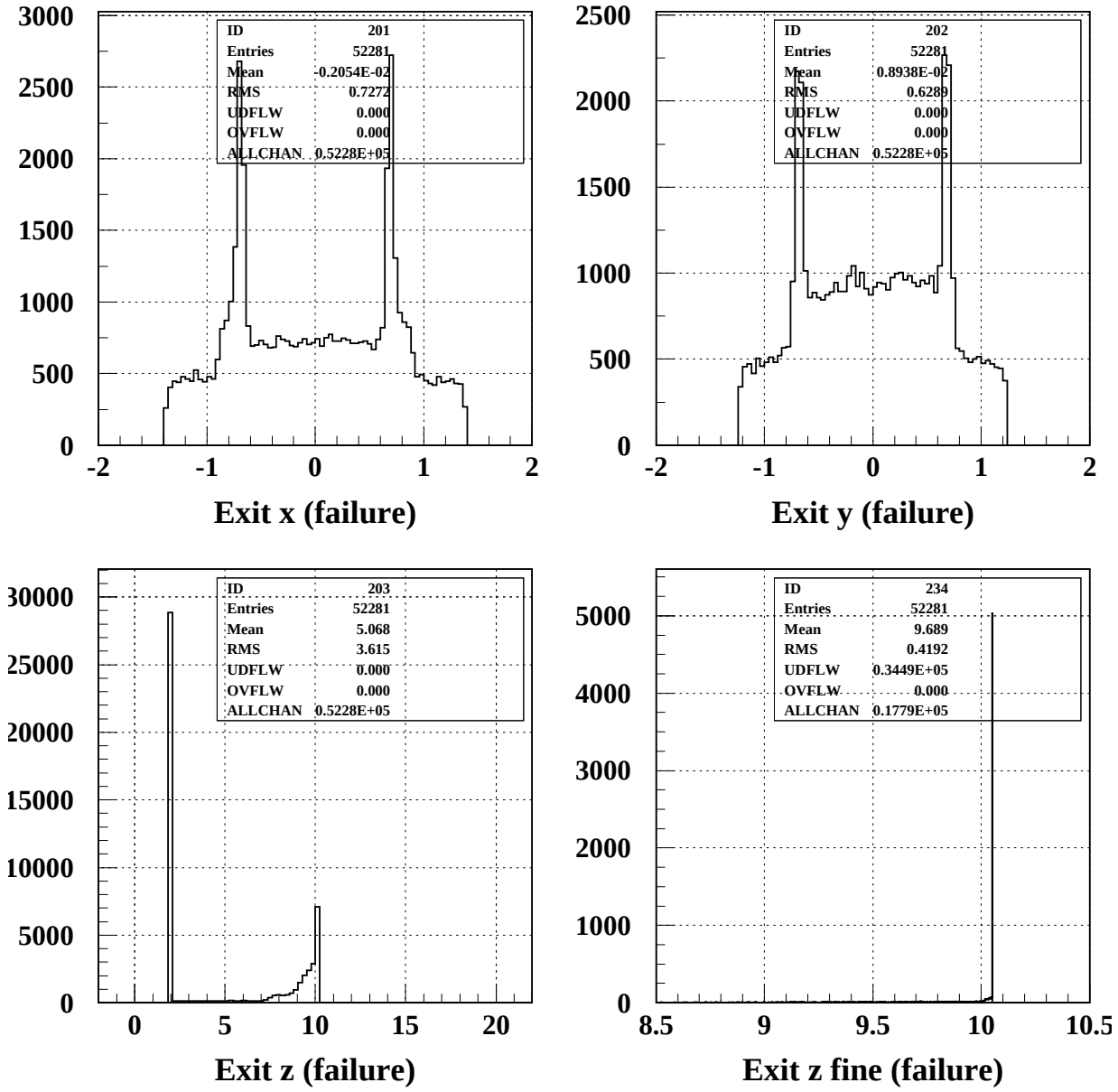

Figure 20: Light Guide #10. Top left) Horizontal distribution of rays that fail to reach the SiPM Top right) Vertical distribution of rays that fail to reach the SiPM. Bottom left) Longitudinal distribution of particles that fail to reach the SiPM. Bottom right) Same as previous on a finer scale.

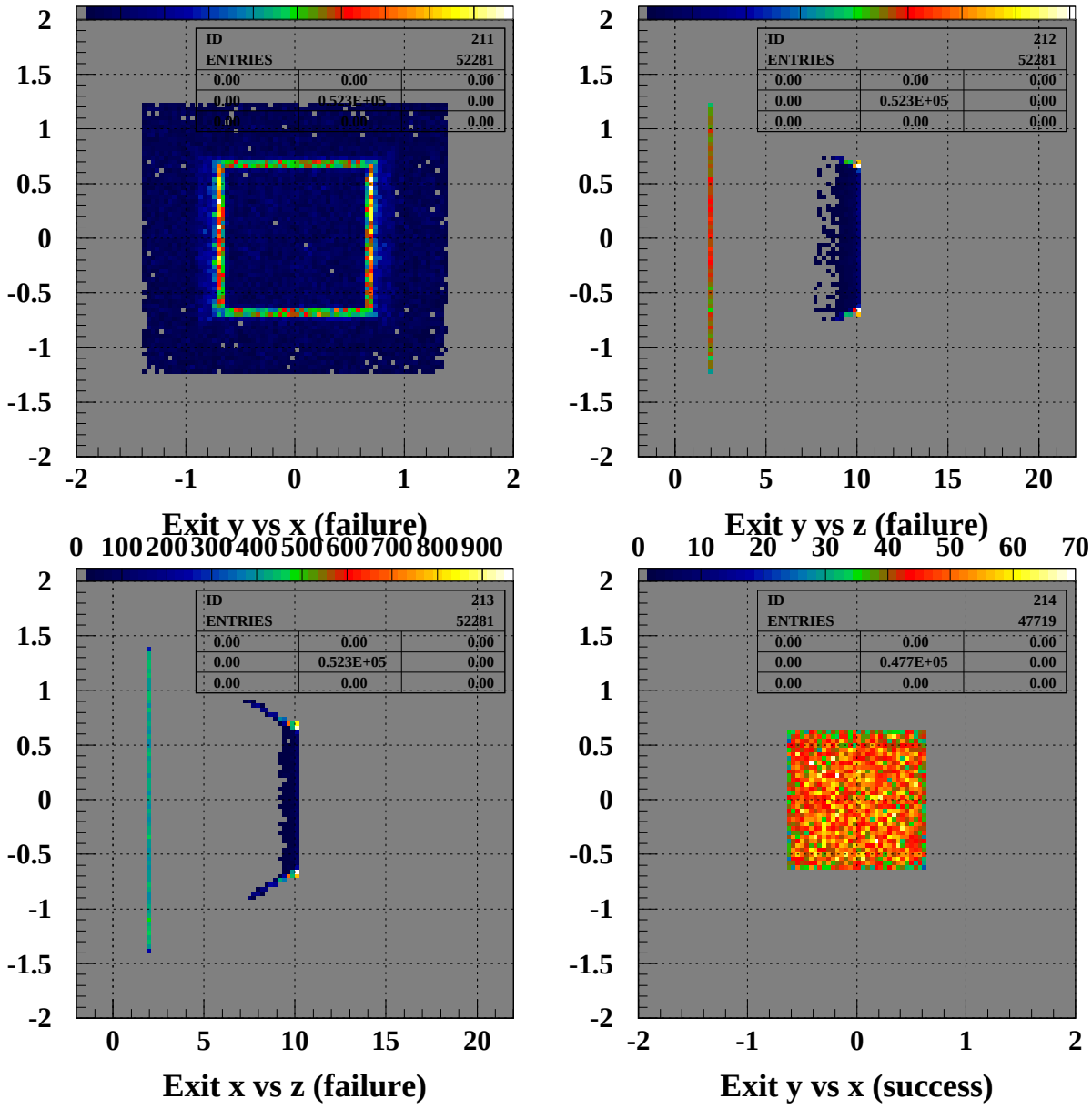

Figure 21: Light Guide #10. Top left) Vertical vs horizontal positions for rays that fail. Top right) Vertical vs longitudinal positions for rays that fail. Bottom left) Horizontal vs longitudinal positions of rays that fail. Bottom right) Vertical vs horizontal positions at the SiPM.

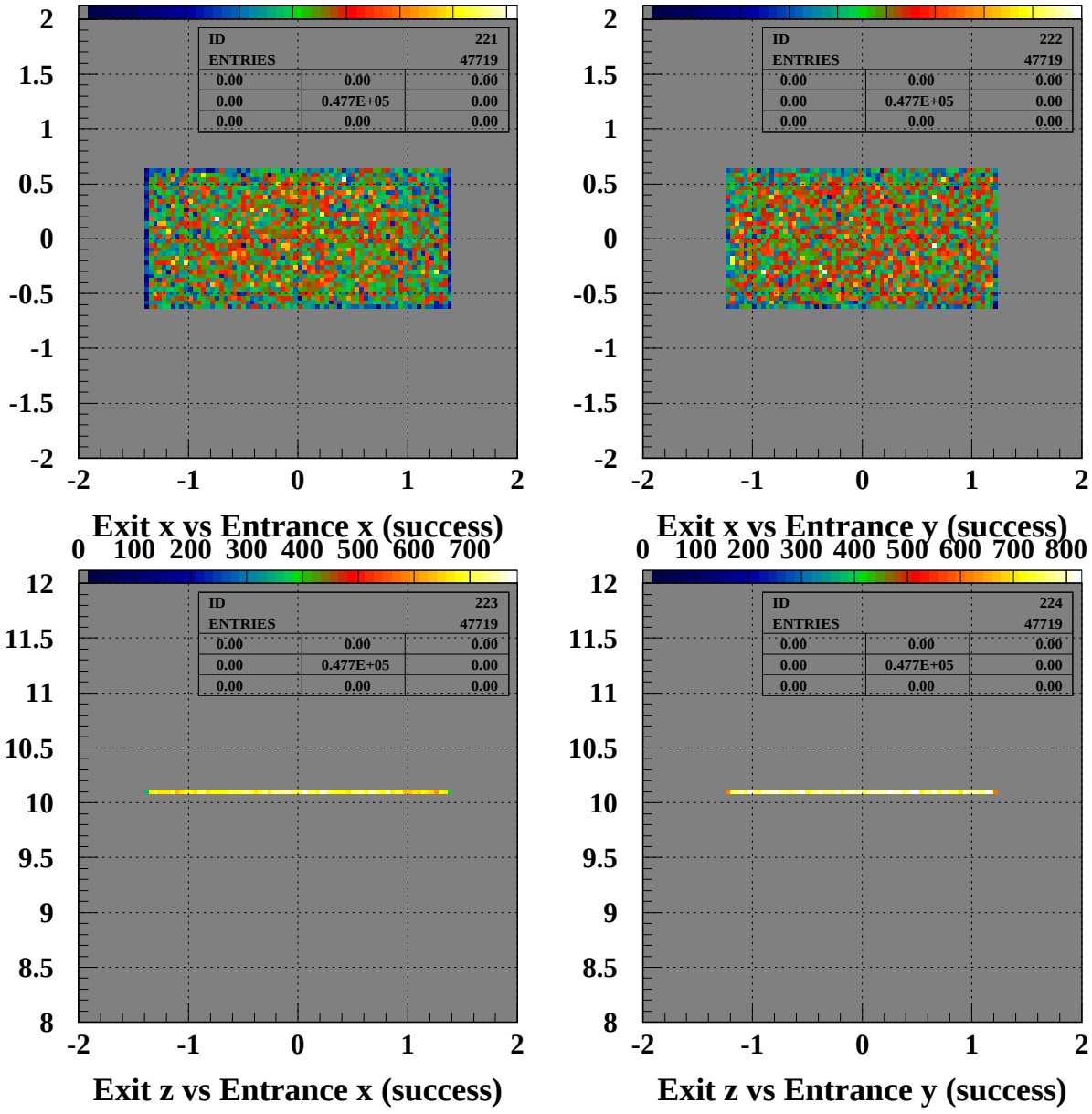

Figure 22: Light Guide #10. Top left) Correlation of horizontal position between entrance and exit. Top right) Correlation of vertical position between entrance and exit. Bottom left) Exit z vs entrance x. Bottom right) Exit z vs entrance y.

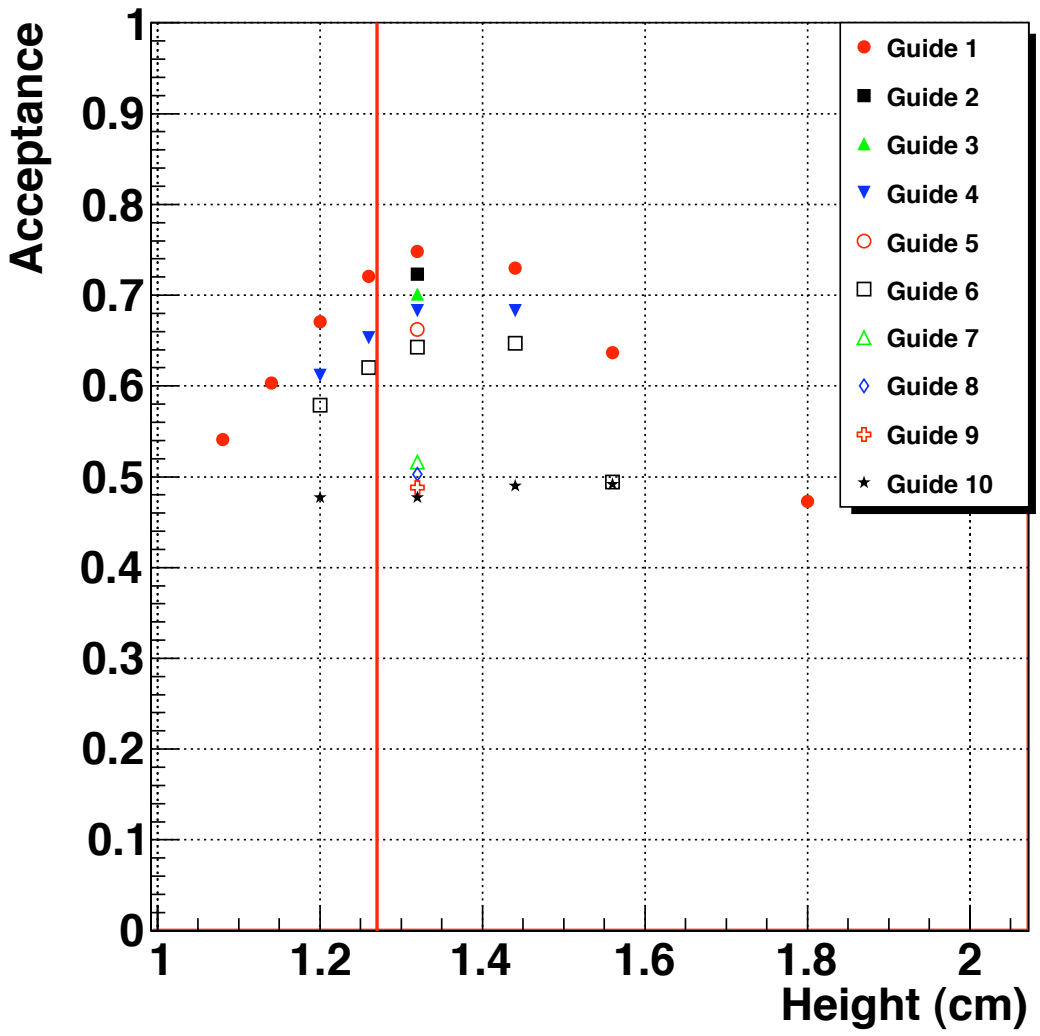

Figure 23: Acceptance as a function of the vertical height of the output face of the light guide.

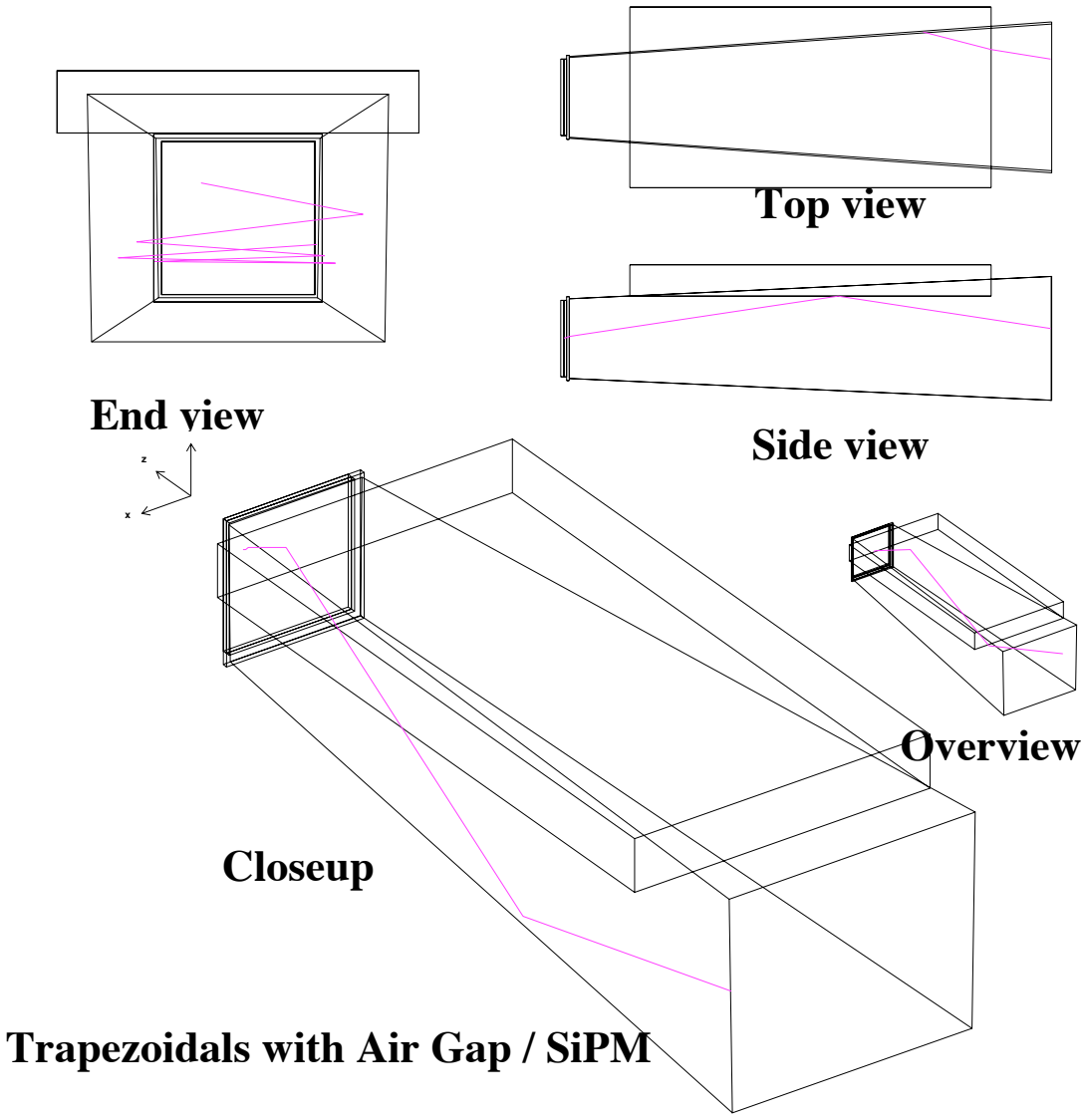

Figure 24: Various views of the geometry for light guide #6 with a step, including rays traced through the guide. The middle right shows the side view with an air volume cutting into the light guide for placing a monitoring board.

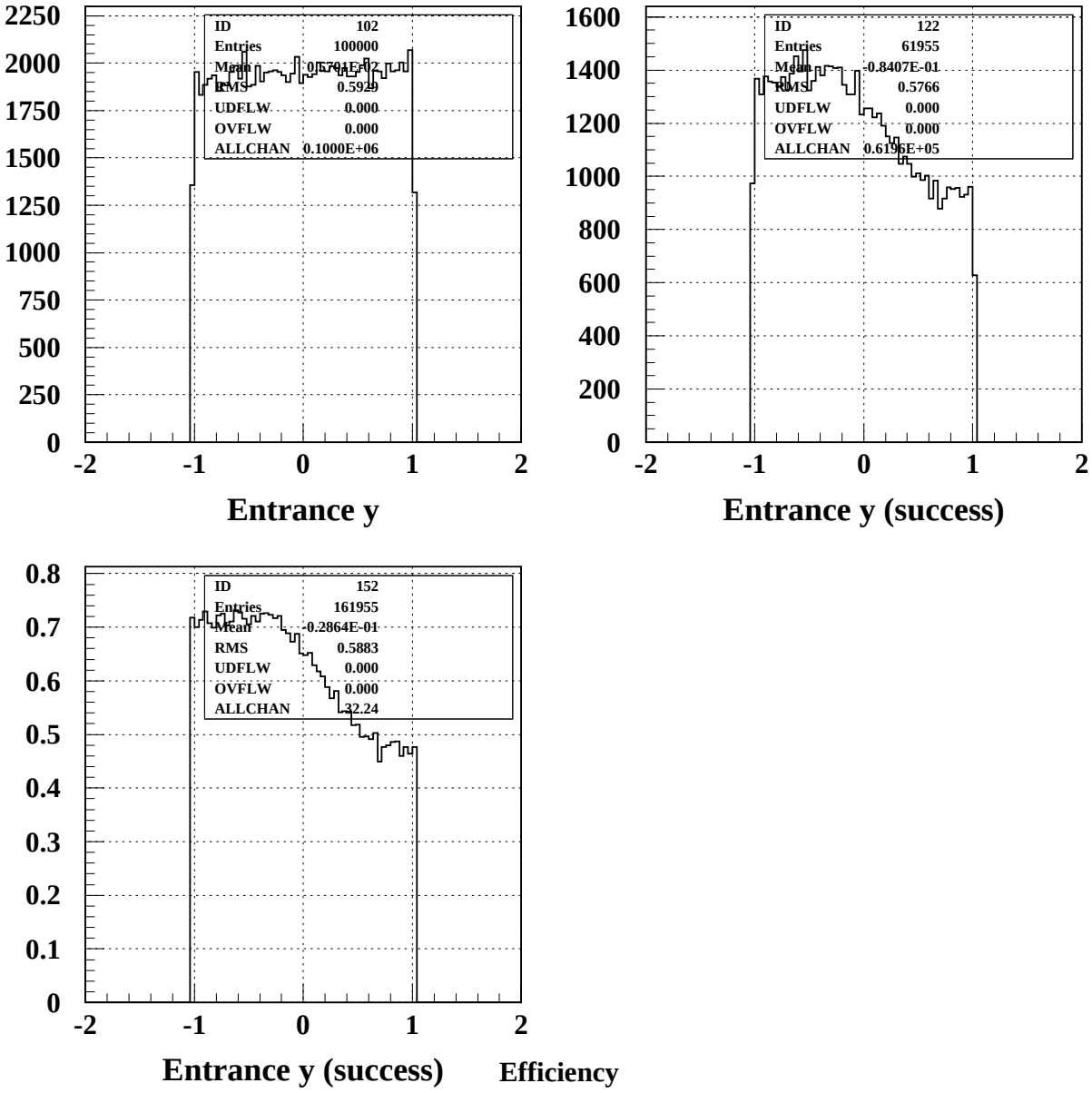

Figure 25: Light Guide #6 with cutout. Top left) Vertical distribution of rays at the entrance. Top right) Vertical distribution of rays that reach the SiPM. Bottom left) Acceptance as a function of vertical position.

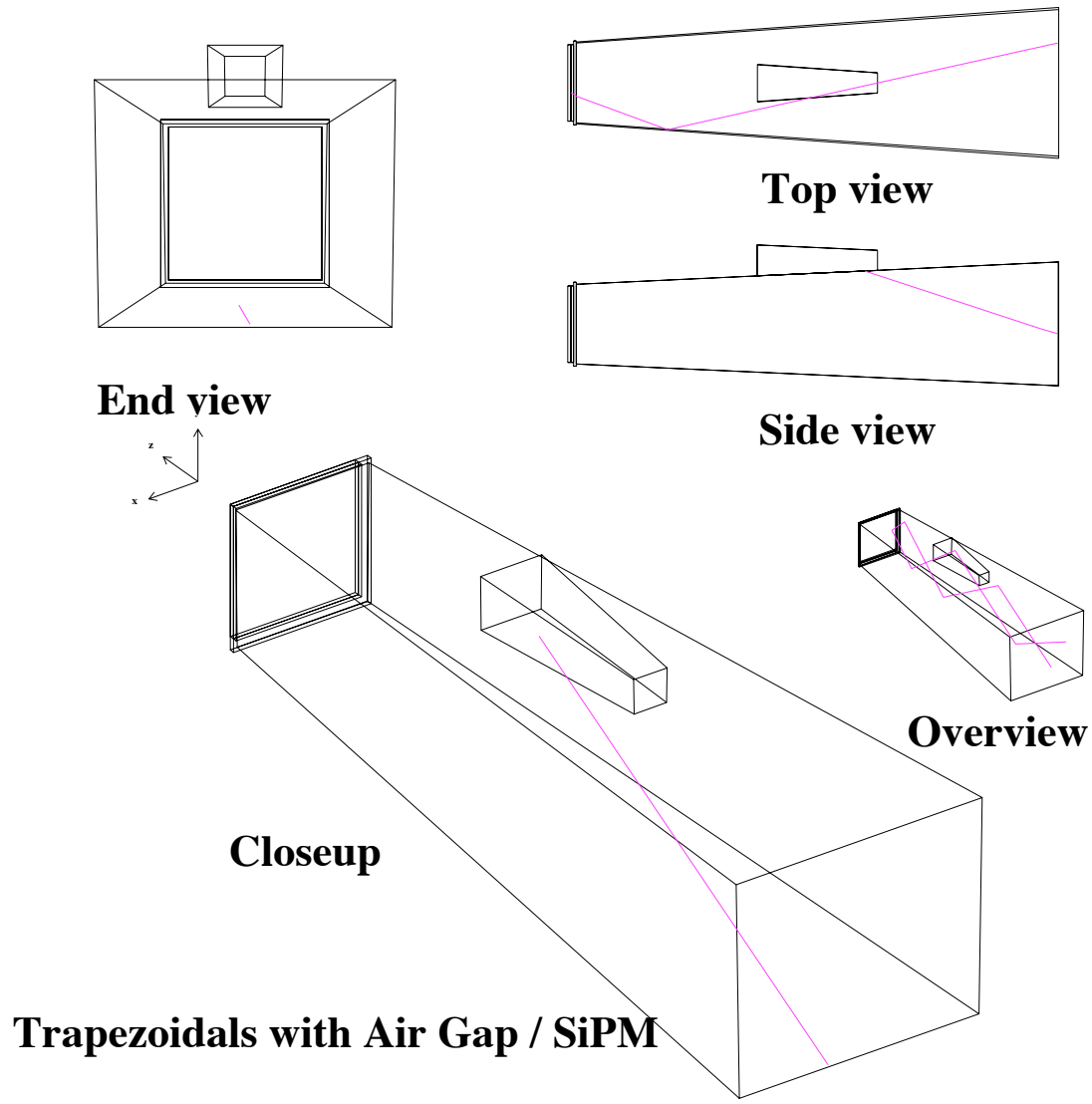

Figure 26: Various views of the geometry for light guide #6 with a patch, including rays traced through the guide. The middle right shows a side view with a carbon patch on the top side. Light rays impinging on the bottom surface of the patch are lost. Note that only the surface in contact with the light guide is relevant to the optics.

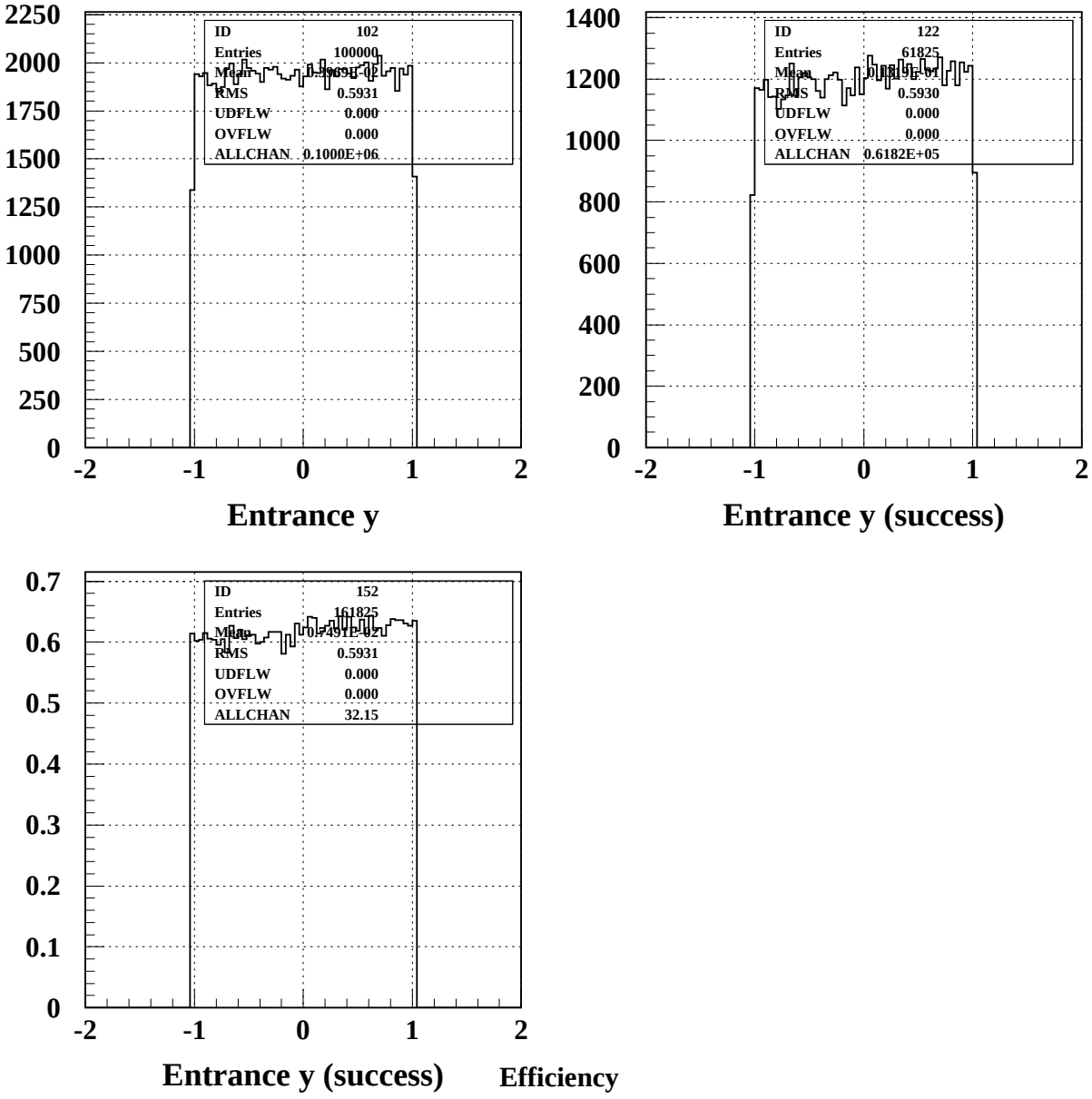

Figure 27: Light Guide #6 with black patch. Top left) Vertical distribution of rays at the entrance. Top right) Vertical distribution of rays that reach the SiPM. Bottom left) Acceptance as a function of vertical position.

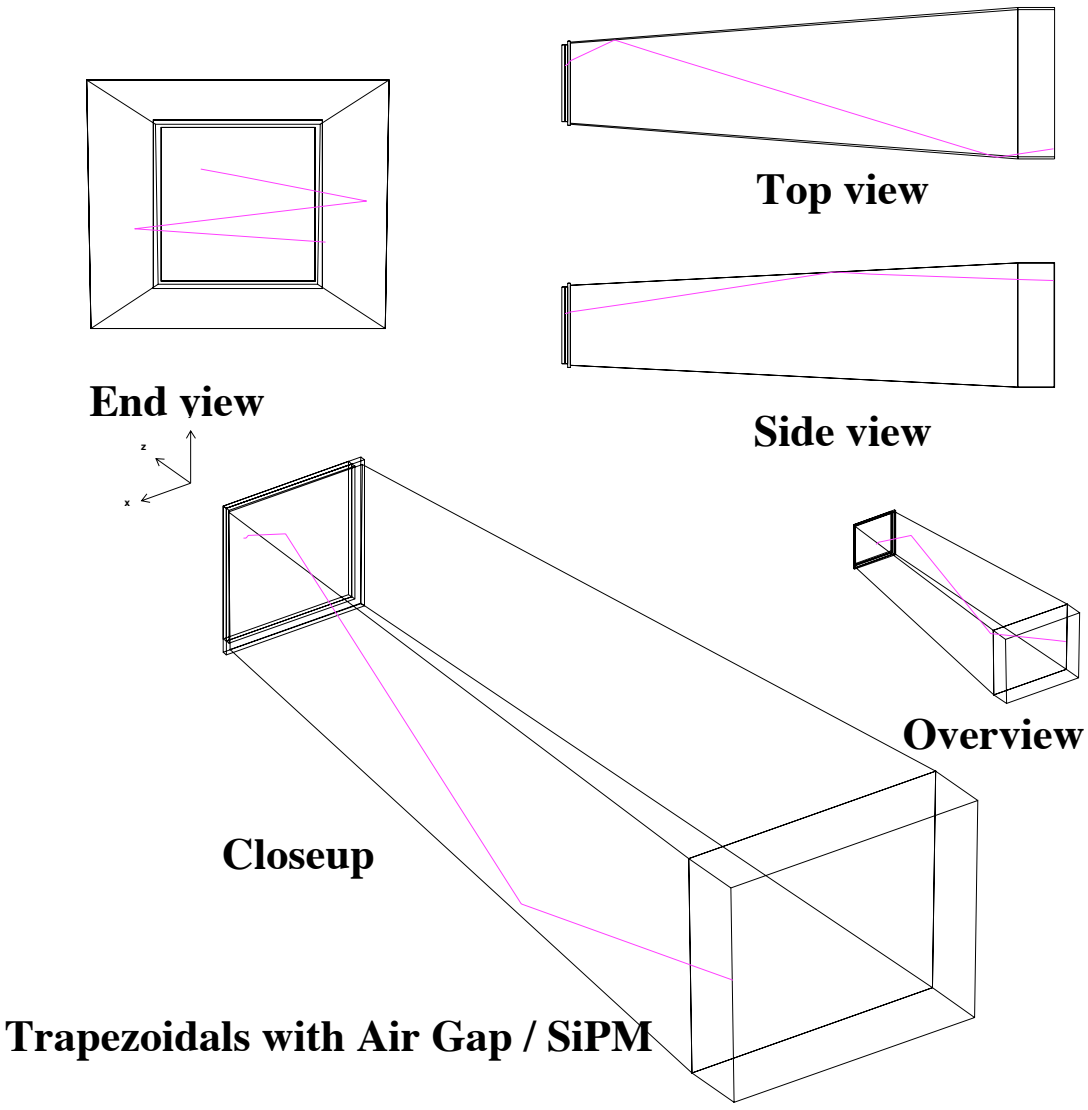

Figure 28: Various views of the geometry for light guide #6 with a 6 mm flat section at the base, including rays traced through the guide. The overall length of the light guide is the nominal 8 cm. Light rays reflecting of the flat sides propagate through the light guide with smaller angles than rays that first reflect of the inclined sides of the light guide.

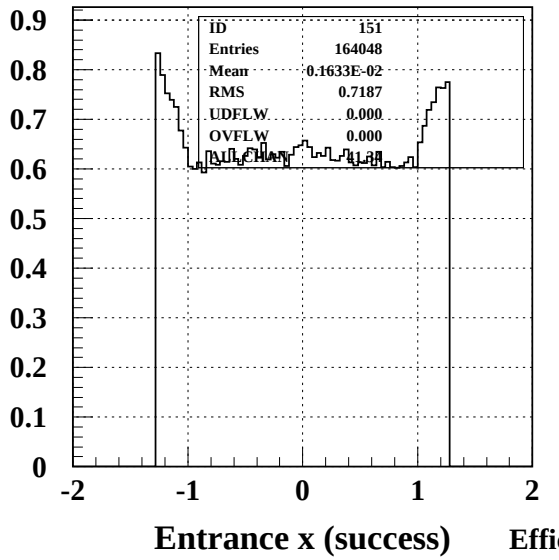

Figure 29: Acceptance as a function of horizontal position for a 6 mm flat section.

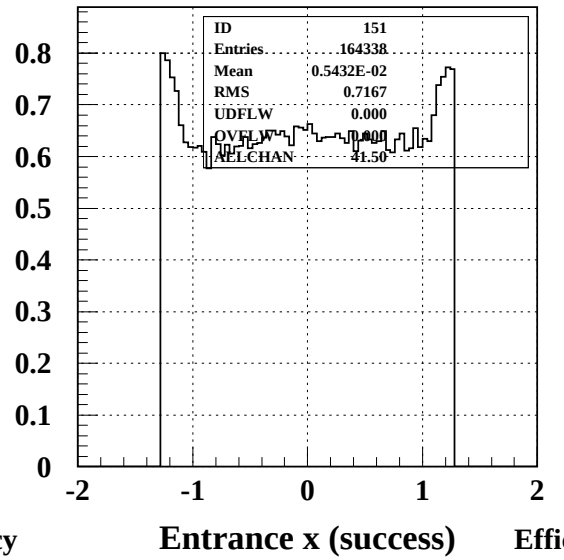

Figure 30: Acceptance as a function of horizontal position for a 4 mm flat section.

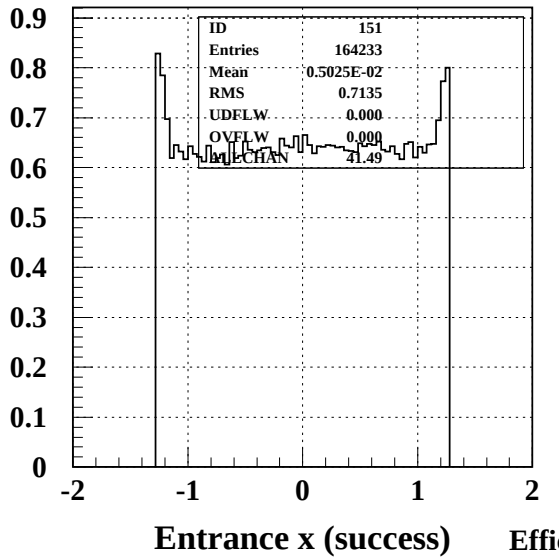

Figure 31: Acceptance as a function of horizontal position for a 2 mm flat section.

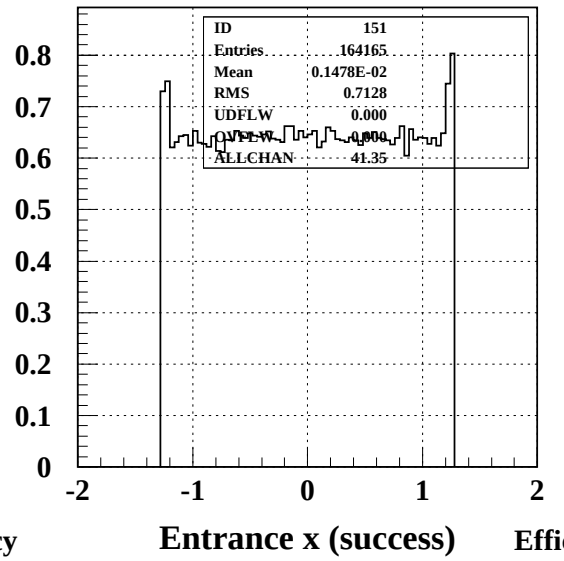

Figure 32: Acceptance as a function of horizontal position for a 1 mm flat section.

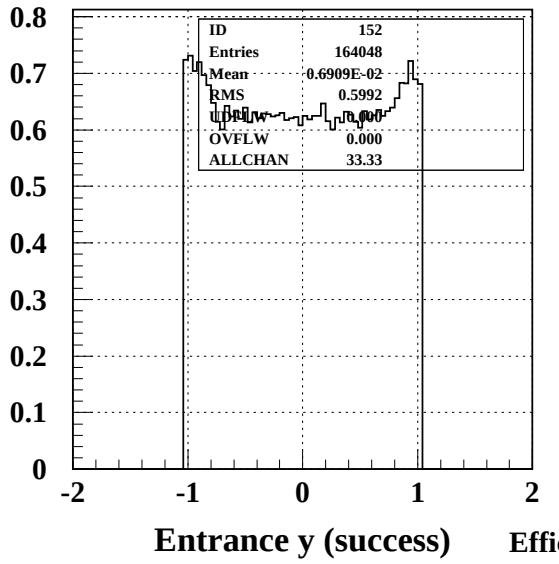

Figure 33: Acceptance as a function of vertical position for a 6 mm flat section.

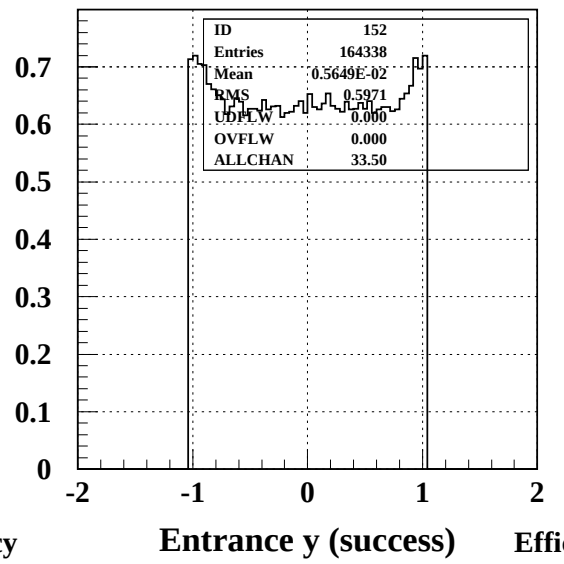

Figure 34: Acceptance as a function of vertical position for a 4 mm flat section.

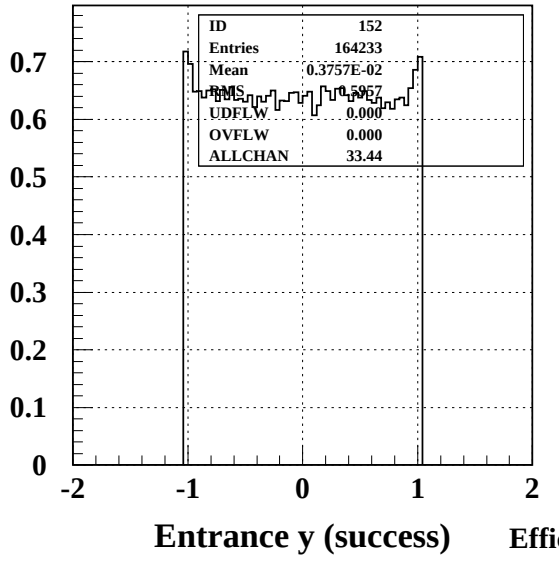

Figure 35: Acceptance as a function of vertical position for a 2 mm flat section.

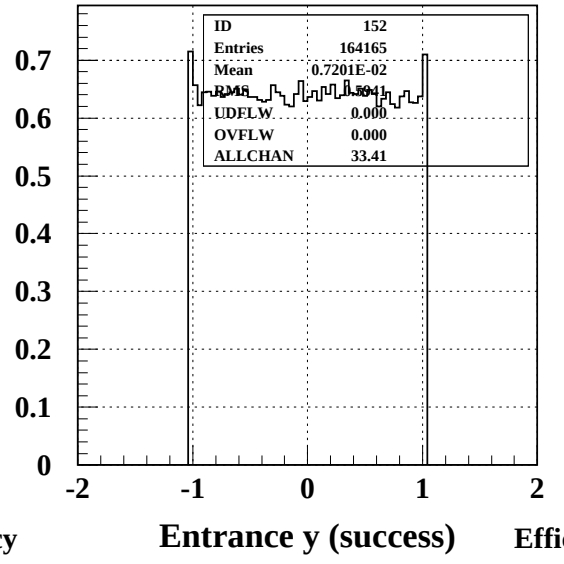

Figure 36: Acceptance as a function of vertical position for a 1 mm flat section.